CDF/ANAL/EXOTIC/CDFR/7260
Version 4.0
October 21, 2011

Baseline Selection of High-p_T Dilepton Events to Search for the Vh Production

Toru Okusawa, Yoshihiro Seiya, Takayuki Wakisaka,

Kazuhiro Yamamoto, and Daisuke Yamato

Osaka City University, Japan

Abstract

This note describes the baseline event selection applied in our like-sign dilepton (ee, $e\mu$, and $\mu\mu$) analysis for the fermiophobic higgs and high-mass Standard-Model higgs searches. The data are extracted from inclusive high-p_T lepton datasets through the so-called `0p.p35` samples, which corresponds to an integrated luminosity of 8.0 fb^{-1} after a good-run selection for the EM calorimeters, muon detectors, and Si vertex detectors. Our base kinematical-cut is $p_T > 20$ GeV/c for the leading lepton (E_T for electrons) and $p_T > 6$ GeV/c for the 2nd lepton. The selection also includes track-quality cuts, isolation cuts, likelihood-based lepton-identification cuts, and minimal requirements on lepton pairs. From the total input of 889 M events, we stripped out 137687 dilepton events.

1 Introduction

Our physics motivation is to search for the neutral higgs boson using events containing a like-sign (LS) dilepton pair produced by the following process:

$$qq' \to Vh \to V(W^*W^*) \to \ell^\pm\ell^\pm + X\ , \qquad V = W,\ Z\ .$$

Relevant higgs mass-regions are above 110 GeV/c^2 for the fermiophobic higgs where the branching fraction of $h \to W^*W^*$ supersedes that of $h \to \gamma\gamma$, and above 160 GeV for the Standard Model higgs where the branching fraction of $h \to b\bar{b}$ is overtaken by this channel.

This note describes the selection of baseline dilepton events to be used in the LS dilepton analysis. Our idea is to select high-p_T isolated dilepton events with less biased but with enough cleanness, and understand them in terms of backgrounds rather than going directly to the final sample which is usually created by highly-optimized selection criteria. We thus allow more events to remain in the sample by keeping kinematical cut on the 2nd leading lepton-leg at minimal. The baseline dilepton events are selected after the lepton selection by imposing very minimal cuts on the lepton pairs. We do not require the charge combination nor apply any Z vetoes at this stage. We will try to understand this miminumly-biased dilepton events through comparisons with background expectations, and gradually proceed to the final LS dilepton events to search for signals.

The selection in the previous analysis is described in [1], where cut-based lepton selections were emplyed. Our analysis now has been expanded to include more recent data corresponding to an integrated luminosity of 8.0 fb^{-1}, and also uses the likelihood-based lepton selection which is the main change from the previous analysis.

2 Datasets and triggers

We expect a high-p_T lepton in the final state because the LS signature requires the on-shell vector-boson produced in association with a higgs to decay leptonically. The Stream-B inclusive high-p_T electron and muon datasets are thus a natural choice for the analysis. The analyzed electron datasets include the `bhel0d, bhel0h, bhel0i, bhel0j, bhel0k, bhel0m,` and `bhel0p` through the period 35, while the muon datasets are the `bhmu0d, bhmu0h, bhmu0i, bhmu0j, bhmu0k, bhmu0m,` and `bhmu0p` through the period 35. The data taking ocurred from 04-Feb-02 to 13-May-11 for these data. More details of the datasets are given in Table 1 taken from the production status WEB page.

From the initial datasets, we perform good-run filtering using the good-run lists of the version 31 or later with the options "silicon" and "CMX ignored". Tables 2–4 show the statistics of event reduction by the good-run filtering. The total integrated luminosity of the input sample is 9.4 fb^{-1}, which becomes 8.0 fb^{-1} after the good-run selection[1] (about 85%). The numbers of runs in the table are actually those seen by the begin-run entry points, thus they are the total numbers including double counting which depends on the data production process.

In the good-run filtering, we also select events coming through specific trigger paths which are

- `ELECTRON_CENTRAL_18_v*`,
- `MUON_CMUP18_v*`,
- `MUON_CMX18_v*`,

and their variants for muon triggers as listed in Tables 5 and 6. They basically require good leptons in the central region with $p_T > 18$ GeV/c. Table 5 also shows how the total number of runs are distributed among the muon triggers if they are shared by different triggers. Main features of the triggers are noted in Table 7. The statistics after

[1]The luminosities after the selection are reflecting the good run-section selection as well. The effect from the run-section selection is however a $< 1\%$ level.

the trigger selection is already included in Tables 2–4. The `CMX` path is only allowed for the runs equal to and after 150145, which corresponds to a loss of the integrated luminosity of 20.1 pb^{-1}.

Figure 1 shows instantaneous luminosities recorded for the events in the electron data. The number of entries in this plot is the same as the number of events after the good-run filtering and the trigger selection. Figure 2 shows a distribution of the number of primary-vertices found in the events of the electron data. Figure 3 shows a z distribution of primary vertices that we choose for our analysis from, as an example, the electron data. We observe similar distributions from the muon data (not shown).

3 Lepton selection

Table 8 lists our event pre-selection and lepton selection cuts. The vertex with the highest p_T-sum of associated tracks, the "h_T vertex", is chosen and required to be within the region to ensure well-defined measurements of collisions by the detector. The leptons we idenfity are checked if they are attached to this primary-vertex. We could have chosen lepton z_0 or the vertex closest to it as our primary vertex, but we do not take that way. The data samples that we use in our analysis do not necessarily contain lepton objects in event, for example, jet samples used to study fake leptons. Formulating the analysis based on the h_T vertex from the beginning provides a consistent treatment of various physics objects throughout the analysis. For vetoing cosmic rays, the standard cosmic-tagger module [2] of the development version is used.

The CEM, CMUP, and CMX are currently allowed for both lepton legs. We require at least one electron with $E_T > 20$ GeV and $p_T > 10$ GeV/c or muon with $p_T > 20$ GeV/c, which is considered to be responsible for firing the triggers we have chosen, and at least one other electron with $E_T > 6$ GeV and $p_T > 6$ GeV/c or muon with $p_T > 6$ GeV/c. The electron variables are mostly obtained by using the `ElectronUser/StdCEMElectron` class. The EM energy correction is applied to the electron E_T, and the lepton momentum is derived with beam-constraint fit. The particular choice of 6 GeV(/c) on the 2nd lepton is rather arbitrary: we just pick up the low-p_T end in fake-lepton studies in a Run-I LS analysis [3].

The impact parameter (d_0) is of course recalculated with respect to the primary vertex. The d_0 cut for electrons might probably be unusual. We make it in the electron selection because we estimate fake-lepton backgrounds using per-track fake rates in the main analysis, and keeping the same track-selection between electrons and muons simplifies the study.

The leptons are required to be isolated in terms of the traditional calorimeter cone-isolation with a cone size of $R = 0.4$ ($\mathrm{ISO}^{\mathrm{cal}}_{0.4}$). Our calorimeter isolation is defined for track objects, and common to both electron and muon candidates. It is

$$\mathrm{ISO}^{\mathrm{cal}}_{0.4} = \sum_{R<0.4} E_T^{(i)} - \left(E_T^{(\mathrm{seed})} + E_T^{(\eta+1)} + E_T^{(\eta-1)} \right) , \tag{1}$$

where $E_T^{(i)}$ is the tower E_T (summed over the EM and hadron calorimeter), $E_T^{(\mathrm{seed})}$ is the E_T of the tower that the track is pointing, and $E_T^{(\eta\pm1)}$ is the same quantities for the towers in the same wedge but with the η index off by 1 with respect to the seed tower. The calorimeter tower object, which practically means the definition of tower η and thus E_T, is constructed by taking the primary-vetex of our choice. The distance R of a tower in the η-ϕ space is calculated around the track by using the EM-tower coordinate.

Details of the likelihood-based lepton selection are described in [4]. As usual, we reject electrons as conversion candidates if an oppositely-charged track satisfying

$$|\delta_{xy}| < 0.2 \text{ cm} \quad \text{and} \quad |\Delta \cot\theta| < 0.04 \tag{2}$$

is found in the track-object list. We are using a private function made by modifying the official `ElectronUser/ConversionFinder.cc` to get additional information from the function. In the conversion veto, we aggressively reject the so-called tridents to minimize charge flips of electrons thus potential LS backgrounds[2].

Figure 4 shows inclusive E_T and p_T spectra for central EM objects with associated track(s) at various selection stages, but with the kinematical cuts turned off to show entire distributions, obtained from the `bhel0d` sample. Figure 5 shows similar plots obtained from the latest data, `bhel0p`, for comparison. The corresponding p_T distributions for muons are shown in Figs. 6 and 7. Figure 8 shows inclusive E_T and p_T spectra for CEM electrons after all the cuts, while the plots for muons are given in Fig. 9. Figure 10 shows η distribution for CEM electrons after all the cuts, and Fig. 11 shows the same one for muons. Figures 12 and 13 show raw $\not\!\!E_T$ and transverse mass for the electron and muon data, respectively, after applying all the lepton selection criteria.

For the events with at least 2 leptons, Fig. 14 shows inclusive E_T and p_T distributions of CEM objects with associated tracks(s) that are found in addition to the leading electron, while Fig. 15 shows p_T distributions of muons found in addition to the leading electron, from the `0d` samples. Figures 16–19 are similar plots but for different types of the leading lepton. The double peaks seen in Fig. 19 for the dimuon events of CMX-CMX type are due to different kinematical regions contributing to the distributions. The one has both muons with same-sign of η (higher p_T), while the other has back-to-back dimuons in terms of the η (lower p_T).

4 Dilepton cuts

For the events with ≥ 2 leptons passing the above selection, we apply the cuts listed in Table 9 to clean up the sample.

The leptons must be consistent with coming from the same vertex, which is an important requirement for dilepton and multi-lepton signatures. We have chosen the primary vertex independent of leptons and each lepton has been already required to

[2]More precisely, we demand the return-code from the finder function to be exactly equal to 0. The case of the error-status code (-1) is thus rejected too.

come from the vertex in the lepton selection, the leptons here are already close to each other at their origins. This cut is therefore merely to enforce desired configuration, not really a new cut.

We require a dilepton mass cut mainly to avoid seeing oniums produced with the rates that we do not understand well. We impose this cut on $e\mu$ pairs too in order to maintain biases the same among all the dilepton types as much as possible.

Categorizing events into ee, $e\mu$, μe, and $\mu\mu$ is done by sorting leptons using track p_T, even for electrons to keep a consistent categorization in fake-electron predictions where we have to rely on track p_T. The $e\mu$ and μe categories respectively represent the 1st (leading) lepton to be an electron and a muon.

To avoid double counts of $e\mu$ or μe events coming from both the electron and muon trigger paths, we match the 1st lepton-type with the path type. Namely, we collect only ee and $e\mu$ events from the electron path, while μe and $\mu\mu$ from the muon path. One implication of this procedure is that the trigger efficiency for $e\mu$ and μe events is made equal to the single-lepton efficiency. Table 10 summarizes the dilepton event-counts as we apply the dilepton cuts. We select 137687 events as the baseline dilepton sample.

Examples of kinematical information of dilepton events that we select are shown in Figs. 20–24 for the 2nd-lepton E_T or p_T distributions after all the baseline dilepton selection, and Figs. 25–33 for dilepton invariant mass distributions.

5 Conclusions

We described updates of the baseline dilepton selection from inclusive high-p_T lepton datasets corresponding to an integrated luminosity of 8.0 fb^{-1}, which we analyze for our neutral higgs search. Our kinematical cut is asymmetric: the high-p_T cut is $E_T > 20$ GeV and $p_T > 10$ GeV/c for electrons, and $p_T > 20$ GeV/c for muons, while the low-p_T cut is $E_T > 6$ GeV and $p_T > 6$ GeV/c for electrons and $p_T > 6$ GeV/c for muons. A calorimeter isolation cut, < 2 GeV, is imposed on both leptons. After applying the likelihood-based lepton identification and minimal dilepton cuts, we selected 137687 dilepton events in the data. We emphasize that these events were basically selected by simple requirements: exactly 2-lepton events that were isolated and of good quality. We did not require a Z veto, nor $\not\!\!E_T$ cut, nor charge-combinations at this stage.

Table 1: List of the analyzed datasets.

Dataset	Period	Run range	Online time	Offline version
0d	0	138425 – 186598	02/04/02 – 08/22/04	5.3.1
0h	1	190697 – 195408	12/07/04 – 03/18/05	6.1.1
	2	195409 – 198379	03/19/05 – 05/20/05	6.1.1
	3	198380 – 201349	05/21/05 – 07/19/05	6.1.1
	4	201350 – 203799	07/20/05 – 09/04/05	6.1.1d
0i	5	203819 – 206989	09/05/05 – 11/09/05	6.1.1d
	6	206990 – 210011	11/10/05 – 01/14/06	6.1.1e
	7	210012 – 212133	01/14/06 – 02/22/06	6.1.1
	8	217990 – 222426	06/09/06 – 09/01/06	6.1.1c_e
	9	222529 – 228596	09/01/06 – 11/22/06	6.1.1c_f
0j	10	228664 – 233111	11/24/06 – 01/31/07	6.1.1c_f
	11	233133 – 237795	01/31/07 – 03/30/07	6.1.1c_f
	12	237845 – 241664	04/01/07 – 05/13/07	6.1.1c_f
	13	241665 – 246231	05/13/07 – 08/04/07	6.1.1c_f
0k	14	252836 – 254683	10/28/07 – 12/03/07	6.1.1c_f
	15	254800 – 256824	12/05/07 – 01/27/08	6.1.1c_f
	16	256840 – 258787	01/27/08 – 02/27/08	6.1.1c_f
	17	258880 – 261005	02/28/08 – 04/16/08	6.1.1c_f
0m	18	261119 – 264071	04/18/08 – 07/01/08	6.1.6, _a, b
	19	264101 – 266513	07/01/08 – 08/24/08	6.1.6_b
	20	266528 – 267718	08/24/08 – 10/04/08	6.1.6_b
	21	268155 – 271047	10/12/08 – 01/01/09	6.1.6_b
	22	271072 – 272214	01/02/09 – 02/10/09	6.1.6_b
	23	272470 – 274055	02/15/09 – 03/21/09	6.1.6_b
	24	274123 – 275848	03/22/09 – 05/04/09	6.1.6_c
	25	275873 – 277511	05/05/09 – 06/13/09	6.1.6_c
	26	282976 – 284843	09/15/09 – 10/25/09	6.1.6_e
	27	284858 – 287261	10/25/09 – 01/05/10	6.1.6_e
	28	287294 – 289197	01/06/10 – 02/25/10	6.1.6_e
0p	29	289273 – 291025	02/26/10 – 04/13/10	6.1.6_f
	30	291294 – 293800	04/13/10 – 06/19/10	6.1.6_f
	31	293826 – 294777	06/20/10 – 07/17/10	6.1.6_f
	32	294778 – 299367	08/21/10 – 11/01/10	6.1.6_f
	33	299368 – 301303	11/01/10 – 12/24/10	6.1.6_f
	34	301952 – 303854	01/06/11 – 03/06/11	6.1.6_f
	35	304266 – 306762	03/12/11 – 05/13/11	6.1.6_f

Table 2: Event reduction by the good-run filtering and trigger selection.

	Runs	Events	L (pb^{-1})	Runs	Events	L (pb^{-1})
		`bhel0d`			`bhmu0d`	
Input	7020	26499561	515.2	3348	6629080	514.7
Good runs & run-sections	4631	17449176	333.0	1954	4096154	333.0
Trigger selection	—	12460505	—	—	3946638	—
		`bhel0h`			`bhmu0h`	
Input	4345	20026640	472.6	1852	5769255	472.6
Good runs & run-sections	3332	15335089	363.0	1313	4452213	363.0
Trigger selection	—	10118837	—	—	4170942	—
		`bhel0i`			`bhmu0i`	
Input	4805	28940435	698.2	2518	8853061	698.2
Good runs & run-sections	4000	24305993	586.7	1974	7311412	586.9
Trigger selection	—	15237448	—	—	5924340	—
		`bhel0j`			`bhmu0j`	
Input	7574	43850838	1032.8	4980	17292745	1032.7
Good runs & run-sections	6907	40097075	944.9	4482	15947103	944.9
Trigger selection	—	23347687	—	—	9687148	—
		`bhel0k`			`bhmu0k`	
Input	5269	37161883	555.6	5177	32847648	555.0
Good runs & run-sections	4617	32775192	484.1	4616	29611807	483.4
Trigger selection	—	11535966	—	—	4725430	—

Table 3: Event reduction by the good-run filtering and trigger selection.

	Runs	Events	L (pb^{-1})	Runs	Events	L (pb^{-1})
		`bhel0m.p18`			`bhmu0m.p18`	
Input	4668	32292122	435.3	4549	30192932	435.4
Good runs & run-sections	3323	22724930	307.1	3218	21337436	307.2
Trigger selection	—	7088739	—	—	2978134	—
		`bhel0m.p19`			`bhmu0m.p19`	
Input	2972	22845526	291.6	2870	20035441	291.4
Good runs & run-sections	2042	16383233	207.7	1979	14356575	207.7
Trigger selection	—	4995401	—	—	2046217	—
		`bhel0m.p20`			`bhmu0m.p20`	
Input	2464	19474015	264.4	2814	18194228	264.4
Good runs & run-sections	2284	17963828	242.7	2637	17002392	242.7
Trigger selection	—	5640672	—	—	2346374	—
		`bhel0m.p21`			`bhmu0m.p21`	
Input	4866	36010466	512.9	4710	29738970	512.8
Good runs & run-sections	4091	30648778	435.2	3857	24975592	435.2
Trigger selection	—	9821522	—	—	4293842	—
		`bhel0m.p22`			`bhmu0m.p22`	
Input	2336	19534244	287.4	1272	8317083	287.4
Good runs & run-sections	2165	18153202	267.0	1171	7758969	267.0
Trigger selection	—	6100075	—	—	2713791	—
		`bhel0m.p23`			`bhmu0m.p23`	
Input	2132	18214804	236.8	1085	6981355	236.9
Good runs & run-sections	1747	15508323	200.8	900	5986658	200.9
Trigger selection	—	5069692	—	—	2020179	—
		`bhel0m.p24`			`bhmu0m.p24`	
Input	2808	22985035	297.6	1312	8267966	297.6
Good runs & run-sections	2376	19468071	252.5	1123	7005851	252.5
Trigger selection	—	6341580	—	—	2551665	—
		`bhel0m.p25`			`bhmu0m.p25`	
Input	2427	18459745	240.8	1143	7378822	240.8
Good runs & run-sections	2139	16198078	211.5	1006	6494459	211.5
Trigger selection	—	5238966	—	—	2114055	—
		`bhel0m.p26`			`bhmu0m.p26`	
Input	1969	14648247	197.0	1082	6314864	197.0
Good runs & run-sections	1595	12235427	164.4	879	5307274	164.4
Trigger selection	—	3984567	—	—	1585252	—
		`bhel0m.p27`			`bhmu0m.p27`	
Input	3723	29565209	430.4	2160	14130797	430.4
Good runs & run-sections	3437	27357475	398.4	2001	13218255	398.4
Trigger selection	—	9490347	—	—	3959130	—
		`bhel0m.p28`			`bhmu0m.p28`	
Input	2637	18030037	275.7	1409	9016428	275.7
Good runs & run-sections	2502	16980679	261.3	1330	8535717	261.3
Trigger selection	—	6154915	—	—	2600748	—

Table 4: Event reduction by the good-run filtering and trigger selection.

	Runs	Events	L (pb^{-1})	Runs	Events	L (pb^{-1})
		`bhel0p.p29`			`bhmu0p.p29`	
Input	3542	26802494	365.7	1839	10885737	365.9
Good runs & run-sections	3202	24649619	336.2	1669	10152251	336.4
Trigger selection	—	8265045	—	—	3352197	—
		`bhel0p.p30`			`bhmu0p.p30`	
Input	5653	34312866	469.5	3588	13261862	469.5
Good runs & run-sections	5206	31972897	437.7	3210	12419739	437.7
Trigger selection	—	10418393	—	—	4353376	—
		`bhel0p.p31`			`bhmu0p.p31`	
Input	2298	13301188	180.4	1172	4352252	180.4
Good runs & run-sections	1777	10320852	139.8	885	3396357	139.8
Trigger selection	—	3318348	—	—	1376846	—
		`bhel0p.p32`			`bhmu0p.p32`	
Input	1660	30363868	455.1	1317	10786174	456.5
Good runs & run-sections	1493	28209461	424.5	1157	10050931	426.0
Trigger selection	—	9536922	—	—	4034235	—
		`bhel0p.p33`			`bhmu0p.p33`	
Input	1257	23838888	382.2	784	8931920	382.2
Good runs & run-sections	1166	22827766	365.5	708	8599424	365.5
Trigger selection	—	8205277	—	—	3447596	—
		`bhel0p.p34`			`bhmu0p.p34`	
Input	1522	28214295	395.9	985	8957798	395.9
Good runs & run-sections	1105	20217539	284.8	705	6430262	284.8
Trigger selection	—	6856309	—	—	2671315	—
		`bhel0p.p35`			`bhmu0p.p35`	
Input	1782	27697780	425.1	1185	8562343	425.1
Good runs & run-sections	1403	22824708	347.7	914	7137450	347.7
Trigger selection	—	7606954	—	—	3088445	—
Total input	79729	593070186	9418.2	53151	295698761	9418.5
Total good runs & run-sections	66540	504607391	7996.5	43688	251584281	7997.9
Total trigger selection	—	196834167	—	—	79987895	—

Table 5: Datasets and selected triggers. The total number of runs containing correponding muon triggers are indicated.

	0d	0h				0i					0j				0k			
Period =	0	1	2	3	4	5	6	7	8	9	10	11	12	13	14	15	16	17
`ELECTRON_CENTRAL_18_v*`	○	○	○	○	○	○	○	○	○	○	○	○	○	○	○	○	○	○
		The total number of good runs																
		1313				1974					4482				4616			
`MUON_CMUP18_v*`	○	○	○	○							○	○	○	○	○	○	○	○
			(962)										(4311)			(4616)		
`MUON_CMUP18_L2_PT15_v*`				○	○	○	○	○	○	○	○	○						
				(351)				(1974)			(1480)							
`MUON_CMUP18_L2_LOOSE_LUMI_260_v*`											○	○						
											(33)							
`MUON_CMUP18_L2_LOOSE_LUMI_240_v*`												○	○					
												(857)						
`MUON_CMUP18_L2_LOOSE_DPS_v*`												○	○	○	○	○	○	○
													(2112)			(4616)		
`MUON_CMUP18_L2_PS10_L3TAG_v*`														○				
														(269)				
`MUON_CMX18_v*`	○	○	○	○													○	○
			(962)														(2564)	
`MUON_CMX18_L2_PT15_v*`				○	○	○	○	○	○	○								
				(351)				(1542)										
`MUON_CMX18_L2_PT15_LUMI_200_v*`										○								
										(219)								
`MUON_CMX18_L2_LOOSE_LUMI_200_v*`										○	○	○	○					
										(213)		(2370)						
`MUON_CMX18_L2_LOOSE_DPS_v*`												○	○	○	○	○	○	○
													(2112)			(4616)		
`MUON_CMX18_LUMI_250_v*`										○	○	○	○					
										(213)		(2370)						
`MUON_CMX18_DPS_v*`												○	○	○	○	○	○	
													(2112)			(2052)		
`MUON_CMX18_L2_PS100_L3TAG_v*`														○				
														(269)				
`MUON_CMX18_L2_PS10_v*`														○		○	○	
														(269)		(1893)		
`MUON_CMX18_L2_PS100_v*`																	○	○
																	(2564)	

Table 6: Datasets and selected triggers.

						0m					
Period =	18	19	20	21	22	23	24	25	26	27	28
ELECTRON_CENTRAL_18_v*	○	○	○	○	○	○	○	○	○	○	○
MUON_CMUP18_v*	○	○	○	○	○	○	○	○	○	○	○
MUON_CMUP18_L2_LOOSE_DPS_v*	○	○	○	○	○	○	○	○	○	○	○
MUON_CMX18_v*	○	○	○	○	○	○	○	○	○	○	○
MUON_CMX18_L2_LOOSE_DPS_v*	○	○	○	○	○	○	○	○	○	○	○
MUON_CMX18_L2_PS100_v*	○	○	○	○	○	○	○	○	○	○	○

				0p			
Period =	29	30	31	32	33	34	35
ELECTRON_CENTRAL_18_v*	○	○	○	○	○	○	○
MUON_CMUP18_v*	○	○	○	○	○	○	○
MUON_CMUP18_L2_LOOSE_DPS_v*	○	○	○	○	○	○	○
MUON_CMX18_v*	○	○	○	○	○	○	○
MUON_CMX18_L2_LOOSE_DPS_v*	○	○	○	○	○	○	○
MUON_CMX18_L2_PS100_v*	○	○	○	○	○	○	○

Table 7: Main features of the selected triggers.

ELECTRON_CENTRAL_18_v*	L1_CEM8_PT8 · Tower $E_T > 8$ GeV · HAD/EM < 0.125 · XFT $p_T > 8.34$ GeV/c	L2_AUTO_L1_CEM8_PT8 · Auto accept. L2_CEM16_PT8 · Cluster $E_T > 16$ GeV · HAD/EM < 0.125 · XFT $p_T > 8$ GeV/c Added during the 0j. · $\|\eta\| < 1.317$ L2_CEM18_PT8 · Cluster $E_T > 18$ GeV	L3_ELECTRON_CENTRAL_18 · $E_T > 18$ GeV · HAD/EM < 0.125 · $p_T > 9$ GeV/c Added during the 0d. · $L_{\rm shr} < 0.4$ · $\|\Delta z_{\rm CES}\| < 8$ cm
MUON_CMUP18_v*	L1_CMUP6_PT4 · CMU $p_T > 6$ GeV/c · CMP $p_T > 3$ GeV/c $\rightarrow$ CMP stub (0d) · XFT $p_T > 4$ GeV/c $\rightarrow$ 4.09 GeV/c (0d)	L2_AUTO_L1_CMUP6_PT4 · Auto accept. L2_TRK8_L1_CMUP6_PT4 (0d) · XFT $p_T > 8.34$ GeV/c L2_CMUP6_PT8 (0d) L2_CMUP6_PT15_3D (0j) · XFT $p_T > 14.77$ GeV/c · Stereo XFT = 1 L2_CMUP6_PT15_3DMATCH (0k) · Stereo XFT = 3	L3_MUON_CMUP_18 · $\|d_x\|_{\rm U} < 10$ cm · $\|d_x\|_{\rm P} < 10$ cm $\rightarrow$ 20 cm (0d) · $p_T > 18$ GeV/c
MUON_CMUP18_L2_PT15_v*	L1_CMUP6_PT4	L2_CMUP6_PT15 · XFT $p_T > 14.77$ GeV/c	L3_MUON_CMUP_18
MUON_CMUP18_L2_LOOSE_LUMI_260_v*	L1_CMUP6_PT4	L2_CMUP6_PT15_LUMI_260 · XFT $p_T > 14.77$ GeV/c · $\mathcal{L} < 260 \times 10^{30}$ cm^{-2}s^{-1}	L3_MUON_CMUP_18
MUON_CMUP18_L2_LOOSE_LUMI_240_v*	L1_CMUP6_PT4	L2_CMUP6_PT15_LUMI_240 · XFT $p_T > 14.77$ GeV/c · $\mathcal{L} < 240 \times 10^{30}$ cm^{-2}s^{-1}	L3_MUON_CMUP_18
MUON_CMUP18_L2_LOOSE_DPS_v*	L1_CMUP6_PT4	L2_CMUP6_PT15_DPS · XFT $p_T > 14.77$ GeV/c · DPS 1–30	L3_MUON_CMUP_18
MUON_CMUP18_L2_PS10_L3TAG_v* (p13 only)	L1_CMUP6_PT4	L2_CMUP6_PT15_3D_ROLXFT_PS10 · XFT $p_T > 14.77$ GeV/c · Stereo XFT = 1 · PS = 10	L3_NULL
MUON_CMX18_v*	L1_CMX6_PT8_PS1 · CMX $p_T > 6$ GeV/c · XFT $p_T > 8$ GeV/c L1_CMX6_PT8_CSX_PS1 (0d) · CMX $p_T > 6$ GeV/c · XFT $p_T > 8.34$ GeV/c · CSX muon L1_CMX6_PT8_CSX (0d) L1_CMX6_PT8_CSX_LUMI_330 · $\mathcal{L} < 330 \times 10^{30}$ cm^{-2}s^{-1}	L2_AUTO_L1_CMX6_PT8 · Auto accept. L2_AUTO_L1_CMX6_PT8_CSX L2_CMX6_PT10 (0d) · XFT $p_T > 10.1$ GeV/c L2_CMX6_PT15_3DMATCH · XFT $p_T > 14.77$ GeV/c · Stereo XFT = 3 L2_CMX6_PT15_3DMATCH_HTDC · REQUIRE_HTDC=1	L3_MUON_CMX18 · $\|d_x\|_{\rm X} < 10$ cm · $p_T > 18$ GeV/c
MUON_CMX18_L2_PT15_v*	L1_CMX6_PT8_CSX	L2_CMX6_PT15 · XFT $p_T > 14.77$ GeV/c	L3_MUON_CMX18
MUON_CMX18_L2_PT15_LUMI_200_v* $\Downarrow$ (0i) MUON_CMX18_L2_LOOSE_LUMI_200_v*	L1_CMX6_PT8_CSX	L2_CMX6_PT15_LUMI_200 · XFT $p_T > 14.77$ GeV/c · $\mathcal{L} < 200 \times 10^{30}$ cm^{-2}s^{-1}	L3_MUON_CMX18
MUON_CMX18_L2_LOOSE_DPS_v*	L1_CMX6_PT8_CSX L1_CMX6_PT8_CSX_LUMI_330	L2_CMX6_PT15_DPS · XFT $p_T > 14.77$ GeV/c · DPS 1–80	L3_MUON_CMX18
MUON_CMX18_LUMI_250_v*	L1_CMX6_PT8_CSX	L2_CMX6_PT15_3D_LUMI_250 · XFT $p_T > 14.77$ GeV/c · Stereo XFT · $\mathcal{L} < 250 \times 10^{30}$ cm^{-2}s^{-1}	L3_MUON_CMX18
MUON_CMX18_DPS_v*	L1_CMX6_PT8_CSX	L2_CMX6_PT15_3D_DPS · XFT $p_T > 14.77$ GeV/c · Stereo XFT · DPS 1–10	L3_MUON_CMX18
MUON_CMX18_L2_PS100_L3TAG_v*	L1_CMX6_PT8_CSX	L2_CMX6_PT15_3D_ROLXFT_PS100 · XFT $p_T > 14.77$ GeV/c · Stereo XFT = 1 · PS = 100	L3_NULL
MUON_CMX18_L2_PS10_v*	L1_CMX6_PT8_CSX	L2_CMX6_PT15_3D_PS10 · XFT $p_T > 14.77$ GeV/c · Stereo XFT = 1 · PS = 10	L3_MUON_CMX18
MUON_CMX18_L2_PS100_v*	L1_CMX6_PT8_CSX L1_CMX6_PT8_CSX_LUMI_330	L2_CMX6_PT15_3D_PS100 · XFT $p_T > 14.77$ GeV/c · Stereo XFT = 1 · PS = 100	L3_MUON_CMX18

Table 8: Event pre-selection and lepton selection cuts.

Electron selection	Muon selection
Event pre-selection	
$\lvert z_{\mathrm{pv}}\rvert < 60$ cm	
Cosmic-ray veto	
Geometrical and kinematical cuts	
CEM	CMUP or CMX
Fiducial	CMU, P: (x,z)-fid $< (0,0)$, $(0,-3)$ cm
	CMX: (x,z)-fid $< (0,-3)$ cm, $\rho_{\mathrm{COT}} > 140$ cm
	Blue-beam veto, keystone veto, miniskirt veto
$E_T^{\ell_1} > 20$ GeV ($p_T > 10$ GeV/c)	$p_T^{\ell_1} > 20$ GeV/c
$E_T^{\ell_2} > 6$ GeV ($p_T > 6$ GeV/c)	$p_T^{\ell_2} > 6$ GeV/c
Track quality cuts	
Axial ≥ 3 and stereo ≥ 2 (≥ 5 hits)	
$\lvert z_0 - z_{\mathrm{pv}}\rvert < 2$ cm	
Silicon hits ≥ 3	
$\lvert d_0\rvert < 0.02$ cm	
Isolation cut	
$\mathrm{ISO}_{0.4}^{\mathrm{cal}} < 2$ GeV	
Identification cuts	
Likelihood based on Z leptons	Likelihood based on Z leptons
· $L > 0.95$	· $L > 0.58$
Other cuts	
Conversion removal	

Table 9: Dilepton selection cuts.

Exactly two leptons
$\lvert z_0^{\ell_1} - z_0^{\ell_2}\rvert < 2$ cm
Dilepton mass > 12 GeV/c^2

Table 10: Number of events passing the dilepton cuts.

0d

	ee	$e\mu$	μe	$\mu\mu$	Total
≥ 2 leptons	4967	25	45	2825	7862
Exactly 2 leptons	4966	25	45	2825	7861
$\lvert z_0^{\ell_1} - z_0^{\ell_2}\rvert < 2$ cm	4965	25	45	2825	7860
Dilepton mass > 12 GeV/c^2	4916	24	44	2702	7686

0h

	ee	$e\mu$	μe	$\mu\mu$	Total
≥ 2 leptons	5394	41	44	3609	9088
Exactly 2 leptons	5394	41	44	3607	9086
$\lvert z_0^{\ell_1} - z_0^{\ell_2}\rvert < 2$ cm	5394	41	44	3607	9086
Dilepton mass > 12 GeV/c^2	5354	41	44	3455	8894

0i

	ee	$e\mu$	μe	$\mu\mu$	Total
≥ 2 leptons	8049	69	74	5501	13693
Exactly 2 leptons	8046	69	74	5500	13689
$\lvert z_0^{\ell_1} - z_0^{\ell_2}\rvert < 2$ cm	8046	69	74	5500	13689
Dilepton mass > 12 GeV/c^2	7987	67	74	5284	13412

0j

	ee	$e\mu$	μe	$\mu\mu$	Total
≥ 2 leptons	10760	69	86	7566	18481
Exactly 2 leptons	10757	69	86	7566	18478
$\lvert z_0^{\ell_1} - z_0^{\ell_2}\rvert < 2$ cm	10757	69	86	7566	18478
Dilepton mass > 12 GeV/c^2	10655	68	85	7238	18046

0k

	ee	$e\mu$	μe	$\mu\mu$	Total
≥ 2 leptons	5747	34	53	3720	9554
Exactly 2 leptons	5745	34	53	3720	9552
$\lvert z_0^{\ell_1} - z_0^{\ell_2}\rvert < 2$ cm	5745	34	53	3718	9550
Dilepton mass > 12 GeV/c^2	5699	33	53	3545	9330

0m

	ee	$e\mu$	μe	$\mu\mu$	Total
≥ 2 leptons	28149	187	229	19812	48377
Exactly 2 leptons	28147	186	228	19810	48371
$\lvert z_0^{\ell_1} - z_0^{\ell_2}\rvert < 2$ cm	28147	186	228	19808	48369
Dilepton mass > 12 GeV/c^2	27914	178	223	18959	47274

0p

	ee	$e\mu$	μe	$\mu\mu$	Total
≥ 2 leptons	20120	117	138	13365	33740
Exactly 2 leptons	20118	117	138	13365	33738
$\lvert z_0^{\ell_1} - z_0^{\ell_2}\rvert < 2$ cm	20114	117	138	13362	33731
Dilepton mass > 12 GeV/c^2	19972	116	135	12822	33045

Total

	ee	$e\mu$	μe	$\mu\mu$	Total
≥ 2 leptons	83186	542	669	56398	140795
Exactly 2 leptons	83173	541	668	56393	140775
$\lvert z_0^{\ell_1} - z_0^{\ell_2}\rvert < 2$ cm	83168	541	668	56386	140763
Dilepton mass > 12 GeV/c^2	82497	527	658	54005	137687

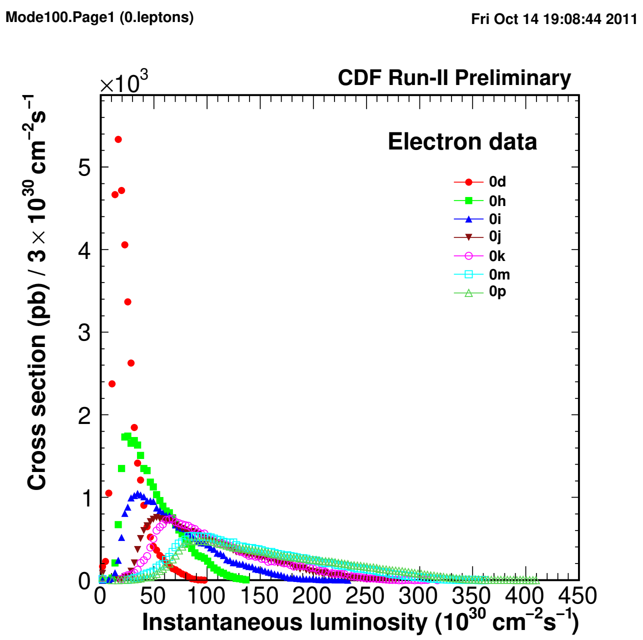

Figure 1: Instantaneous luminosities.

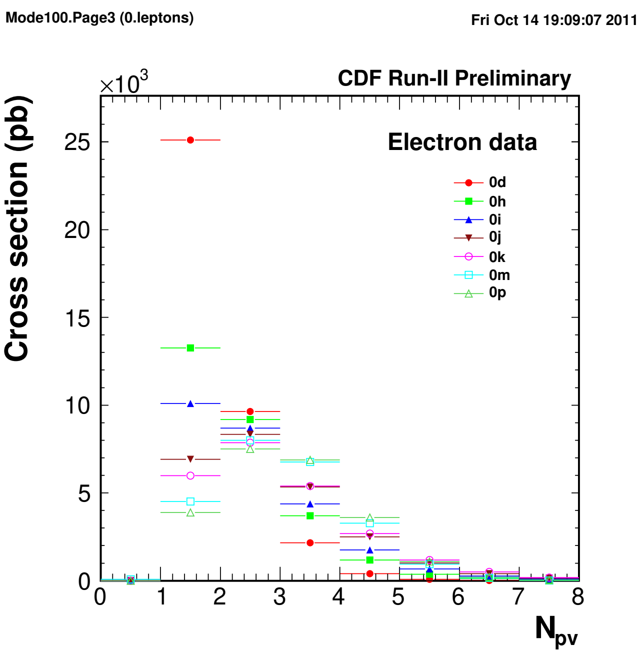

Figure 2: The number of primary vertices.

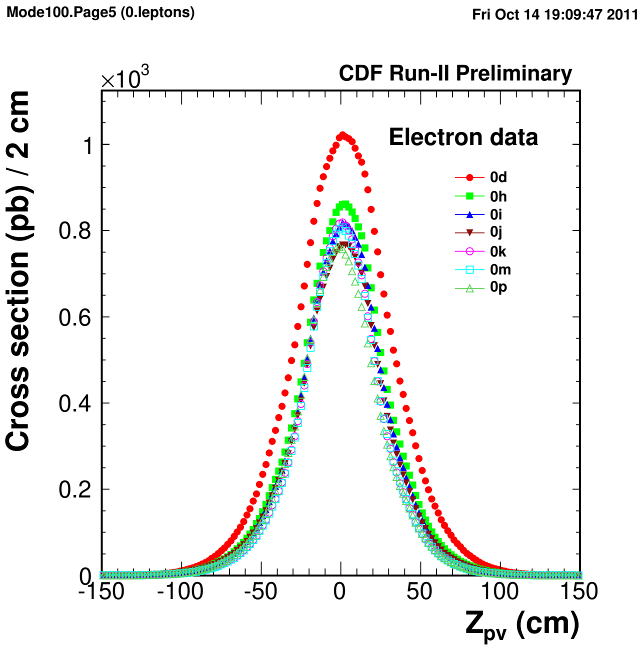

Figure 3: Primary-vertex z distribution.

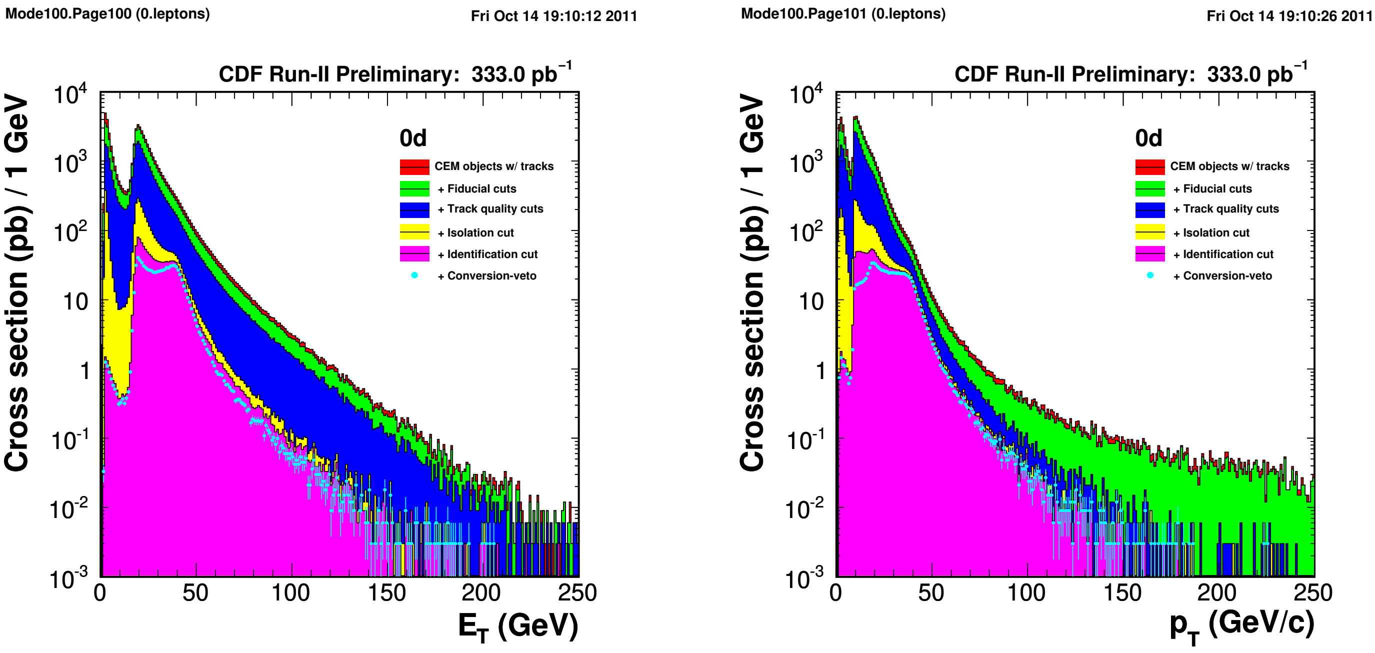

Figure 4: Inclusive E_T (left) and p_T (right) spectra for CEM objects with associated track(s) from the `bhel0d` dataset.

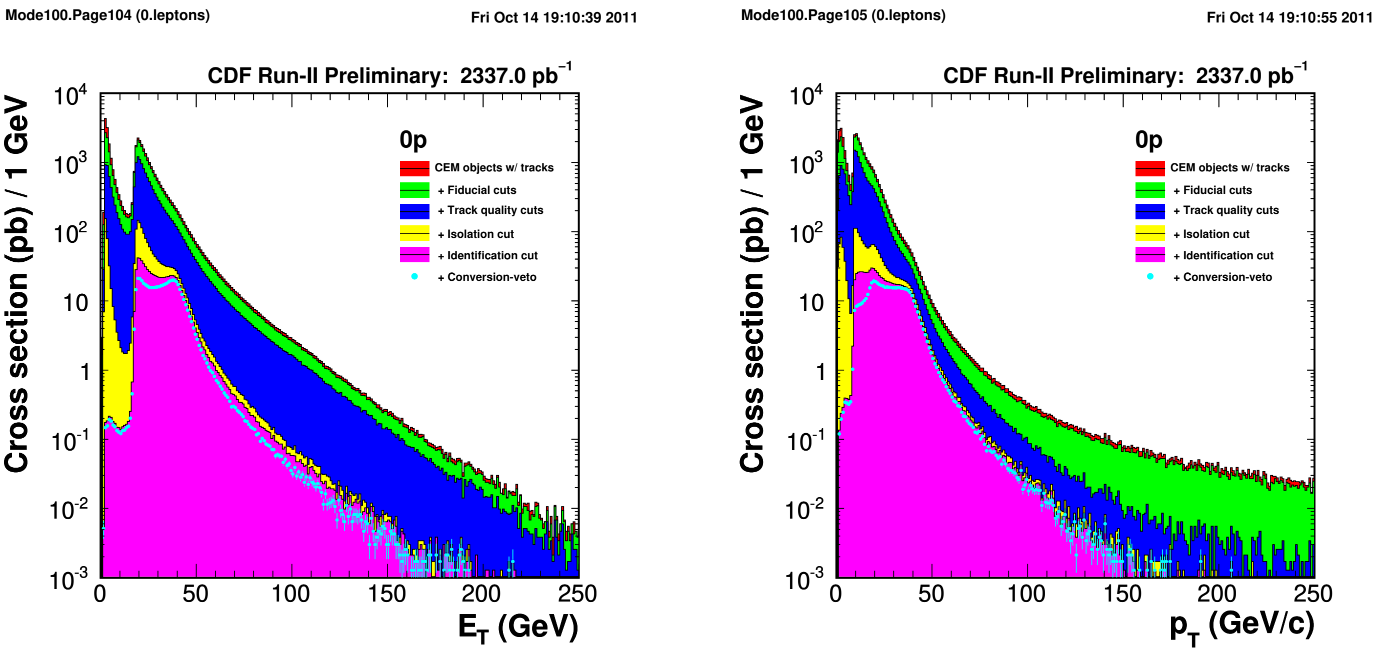

Figure 5: Inclusive E_T (left) and p_T (right) spectra for CEM objects with associated track(s) from the `bhel0p` dataset.

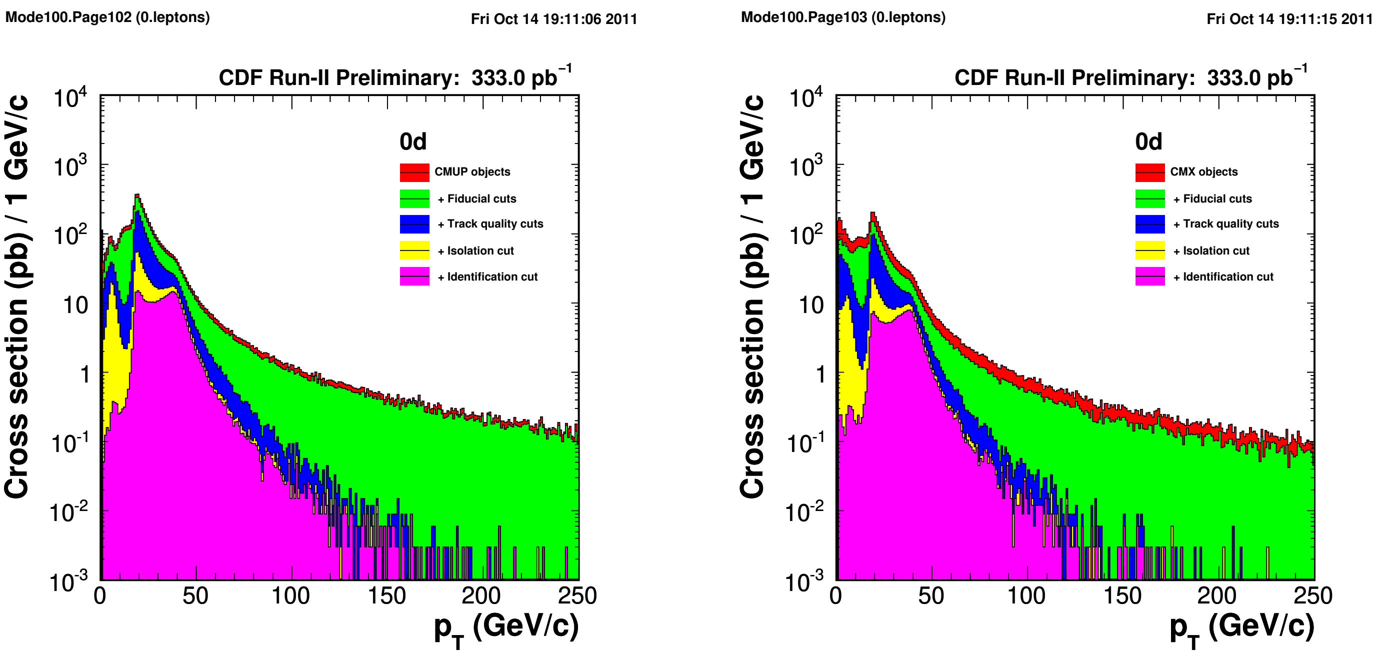

Figure 6: Inclusive p_T spectra for CMUP objects (left) and CMX objects (right) from the `bhmu0d` dataset.

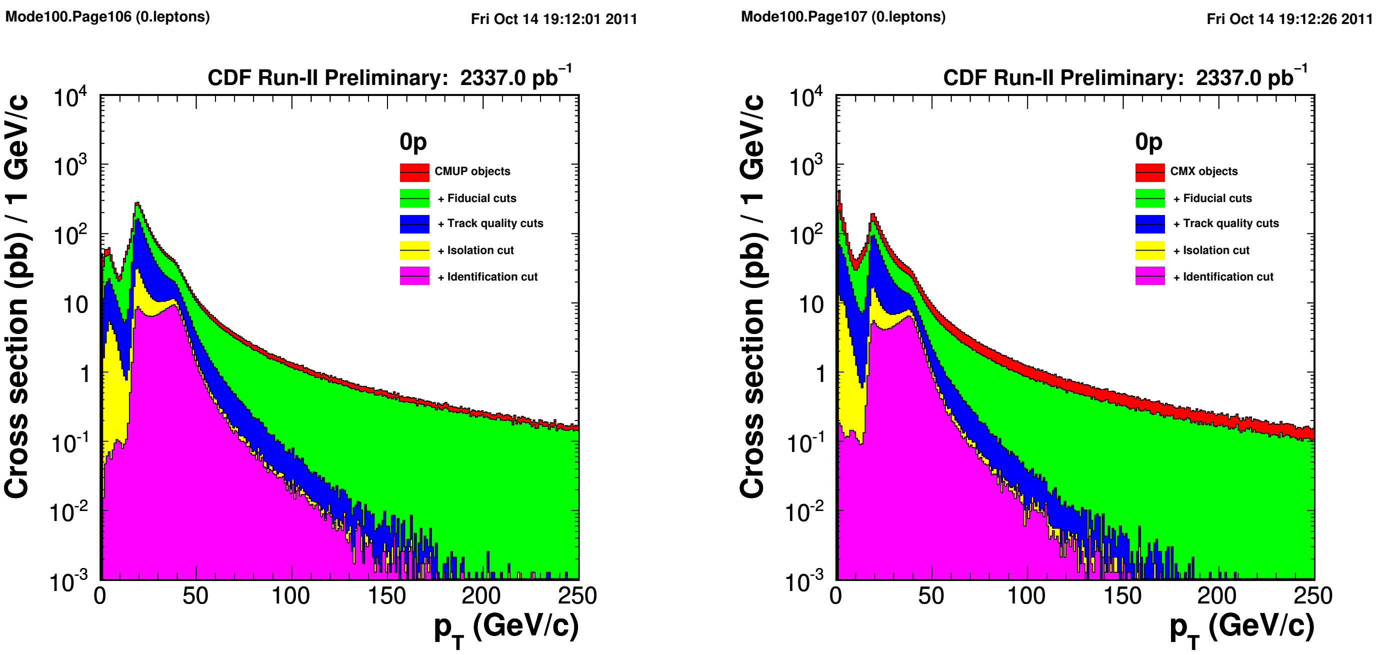

Figure 7: Inclusive p_T spectra for CMUP objects (left) and CMX objects (right) from the `bhmu0p` dataset.

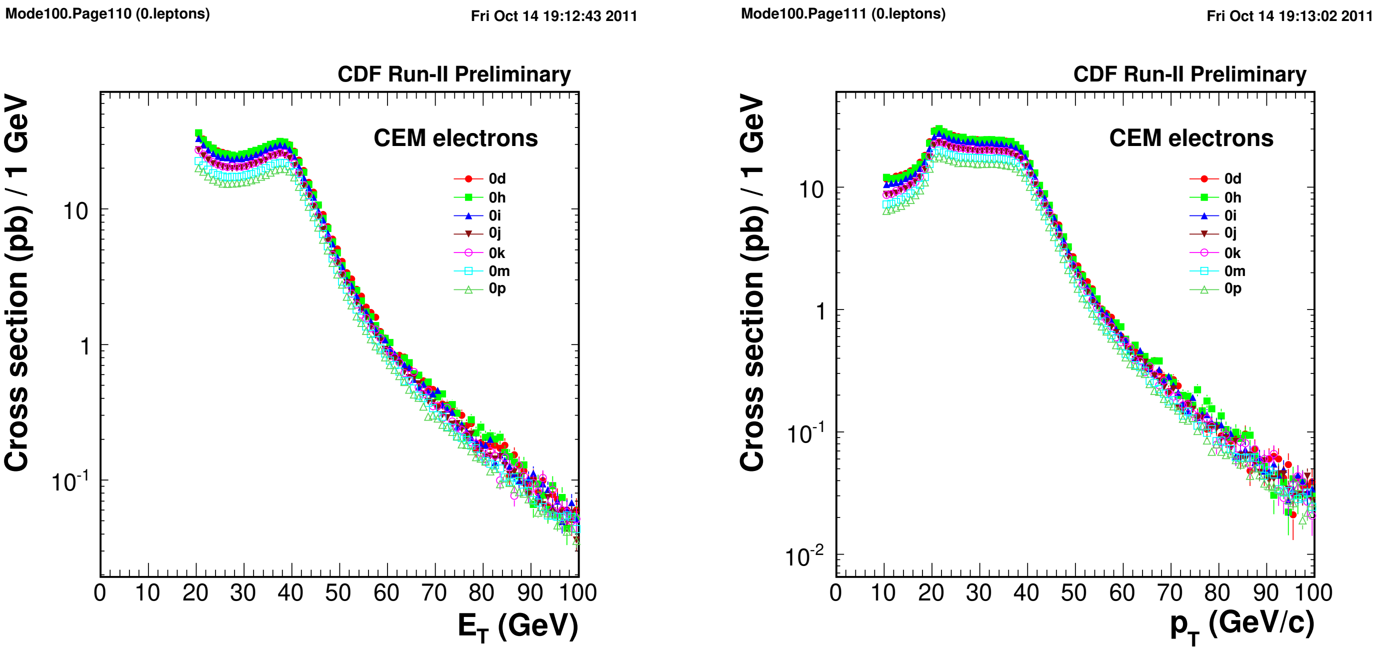

Figure 8: Inclusive E_T (left) and p_T (right) spectra for CEM electrons after all the lepton selection cuts.

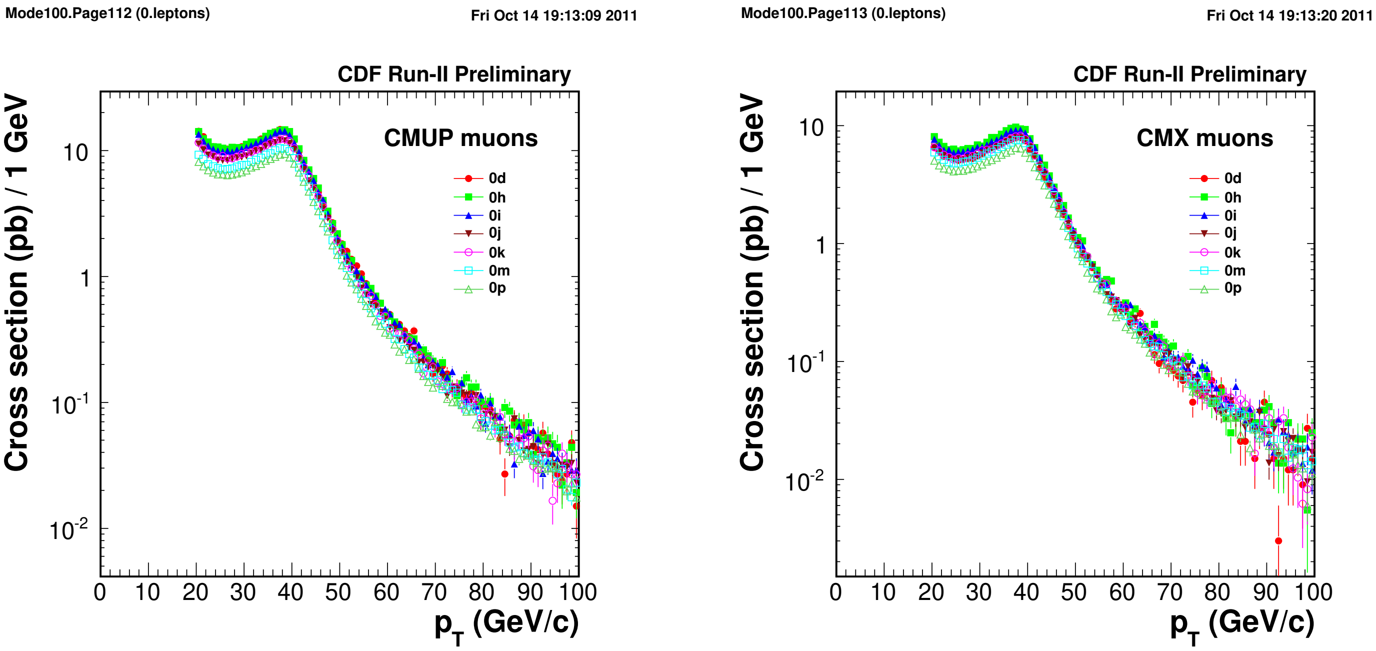

Figure 9: Inclusive p_T spectra for CMUP muons (left) and CMX (muons) after all the lepton selection cuts.

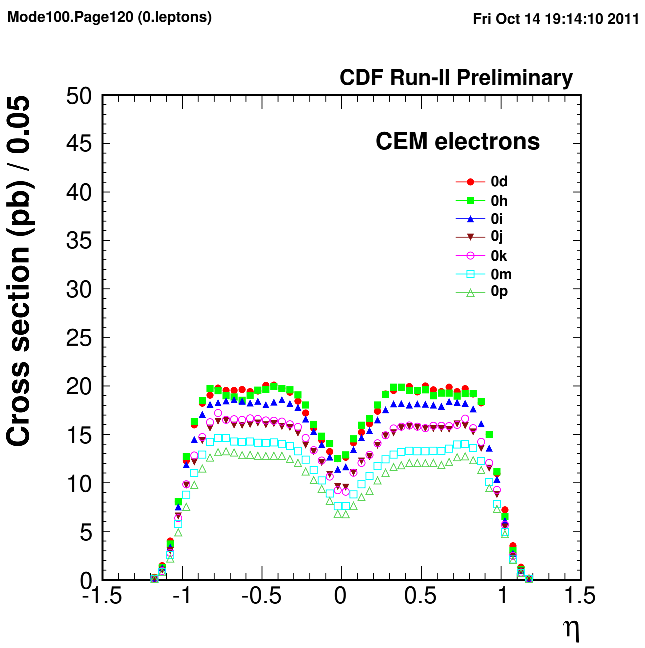

Figure 10: Distribution of the η for CEM electrons after all the lepton selection cuts.

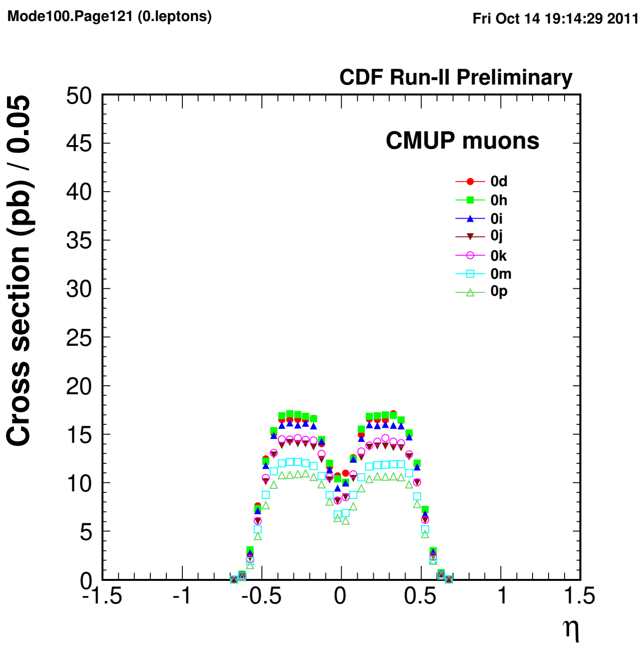

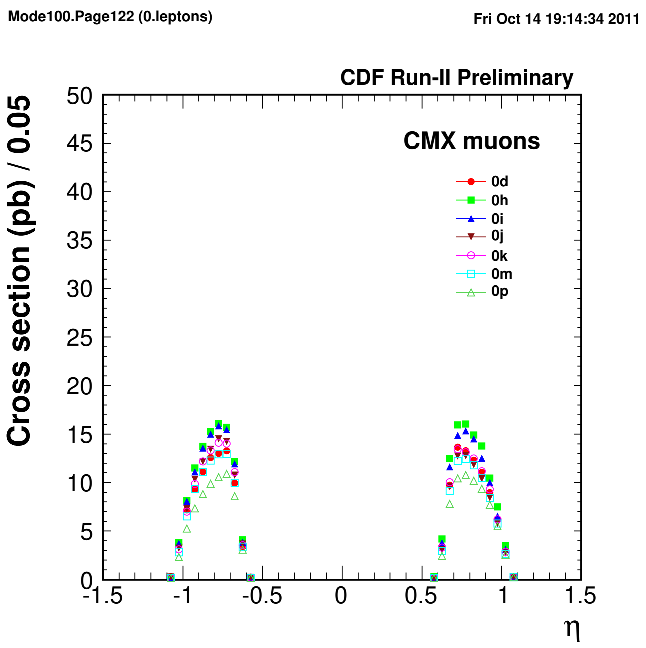

Figure 11: Distributions of the η for CMUP muons (left) and CMX muons (right) after all the lepton selection cuts.

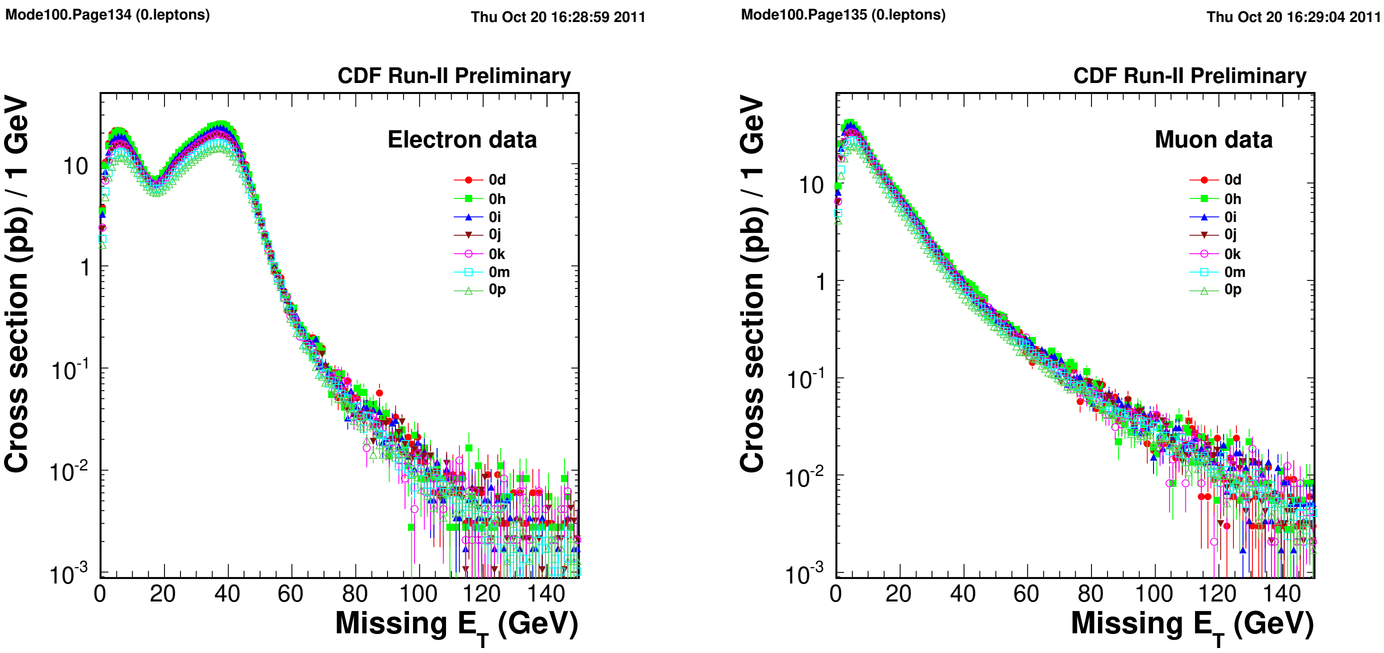

Figure 12: Raw missing E_T distributions for the electron data (left) and the muon data (right) after all the lepton selection cuts.

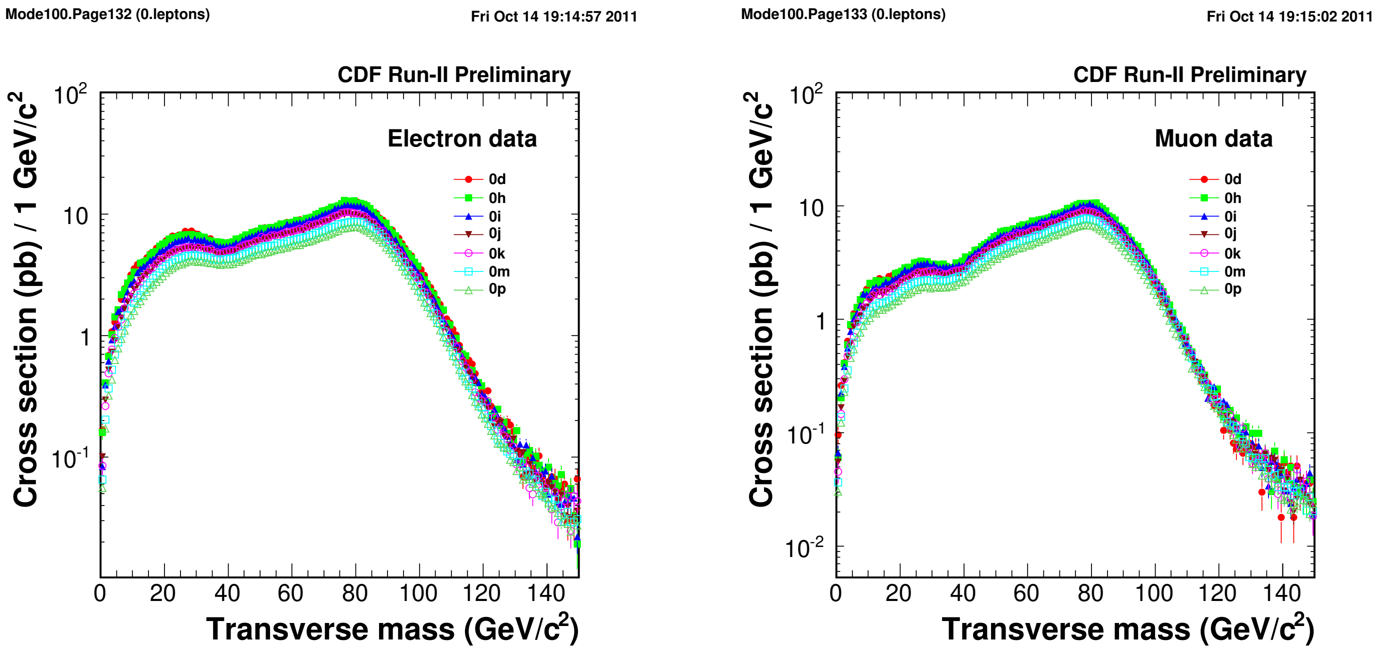

Figure 13: Transverse mass distributions for the electron data (left) and the muon data (right) after all the lepton selection cuts.

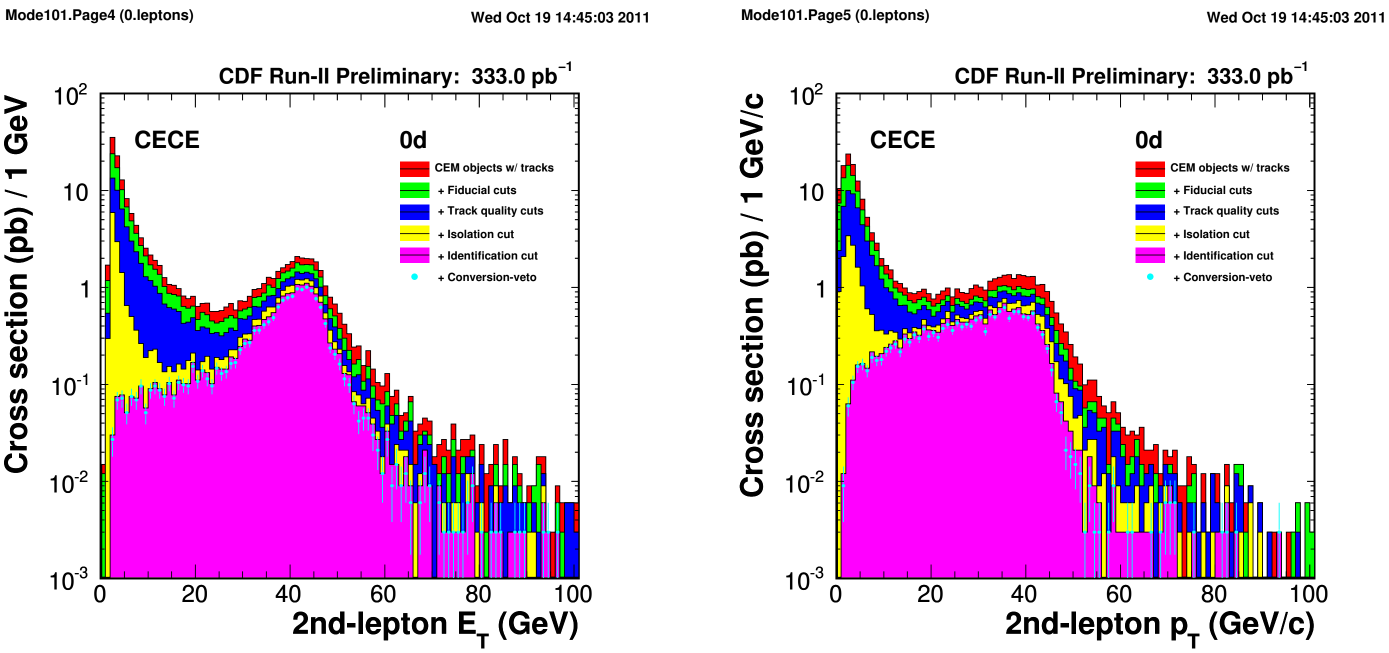

Figure 14: Inclusive E_T (left) and p_T (right) spectra for CEM objects with associated track(s) that are found in addition to the leading electron from the `bhel0d` dataset.

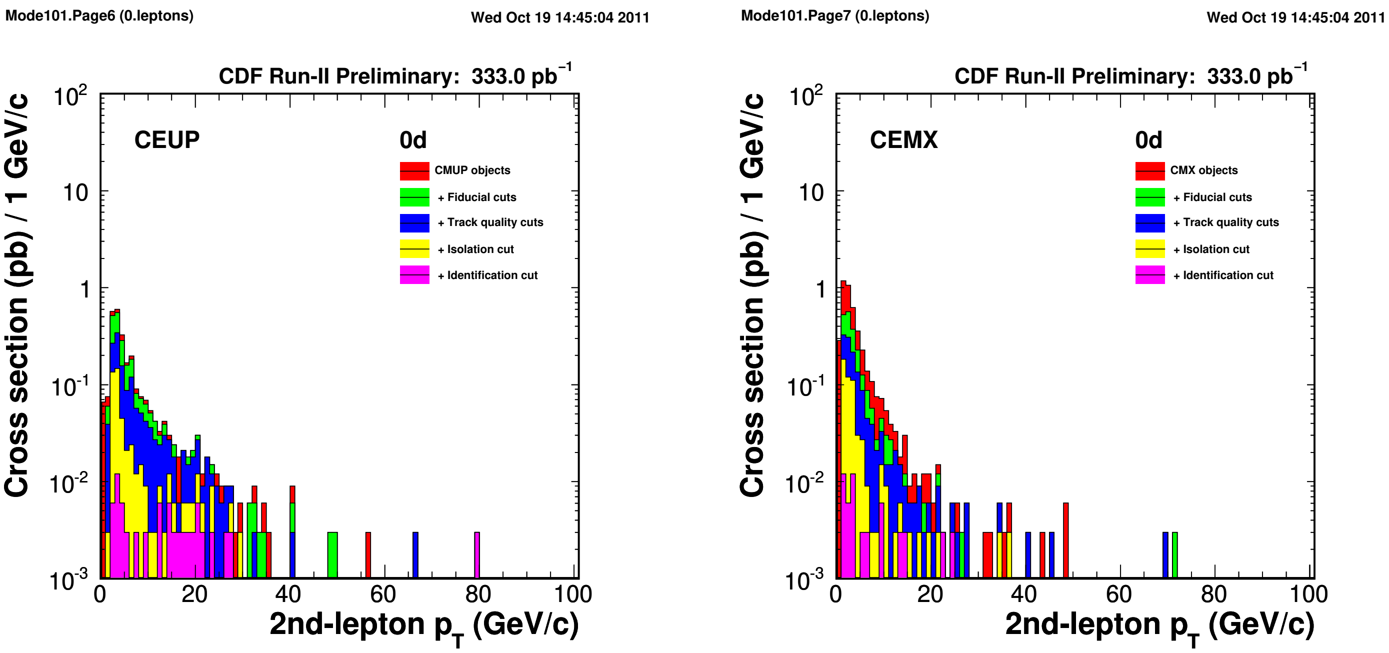

Figure 15: Inclusive p_T spectra for CMUP (left) and CMX (right) objects that are found in addition to the leading electron from the `bhel0d` dataset.

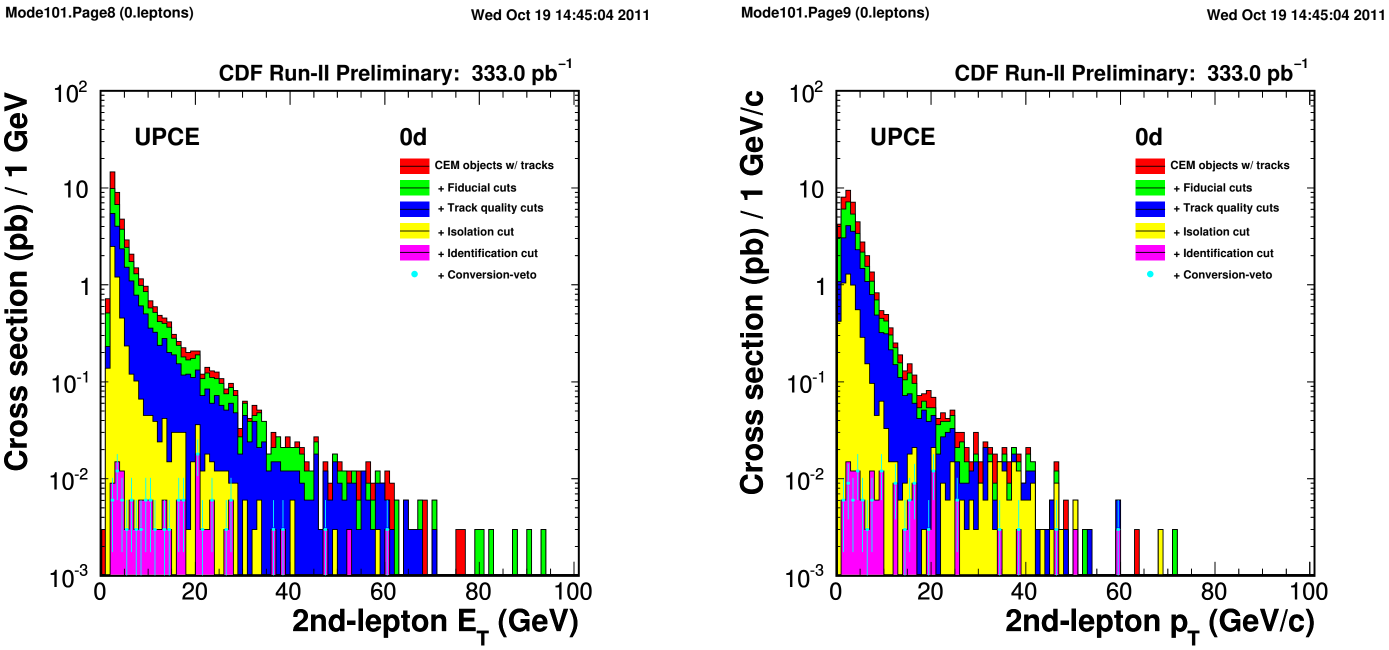

Figure 16: Inclusive E_T (left) and p_T (right) spectra for CEM objects with associated track(s) that are found in addition to the leading CMUP muon from the bhmu0d dataset.

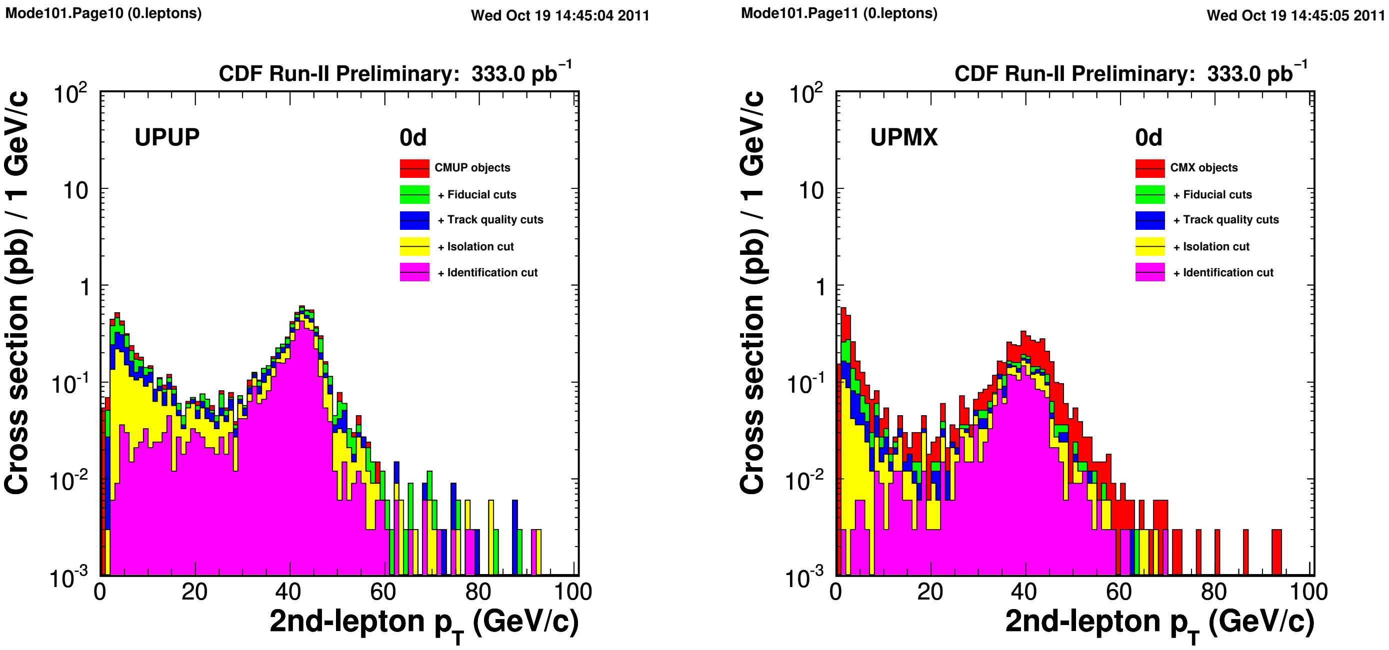

Figure 17: Inclusive p_T spectra for CMUP (left) and CMX (right) objects that are found in addition to the leading CMUP muon from the bhmu0d dataset.

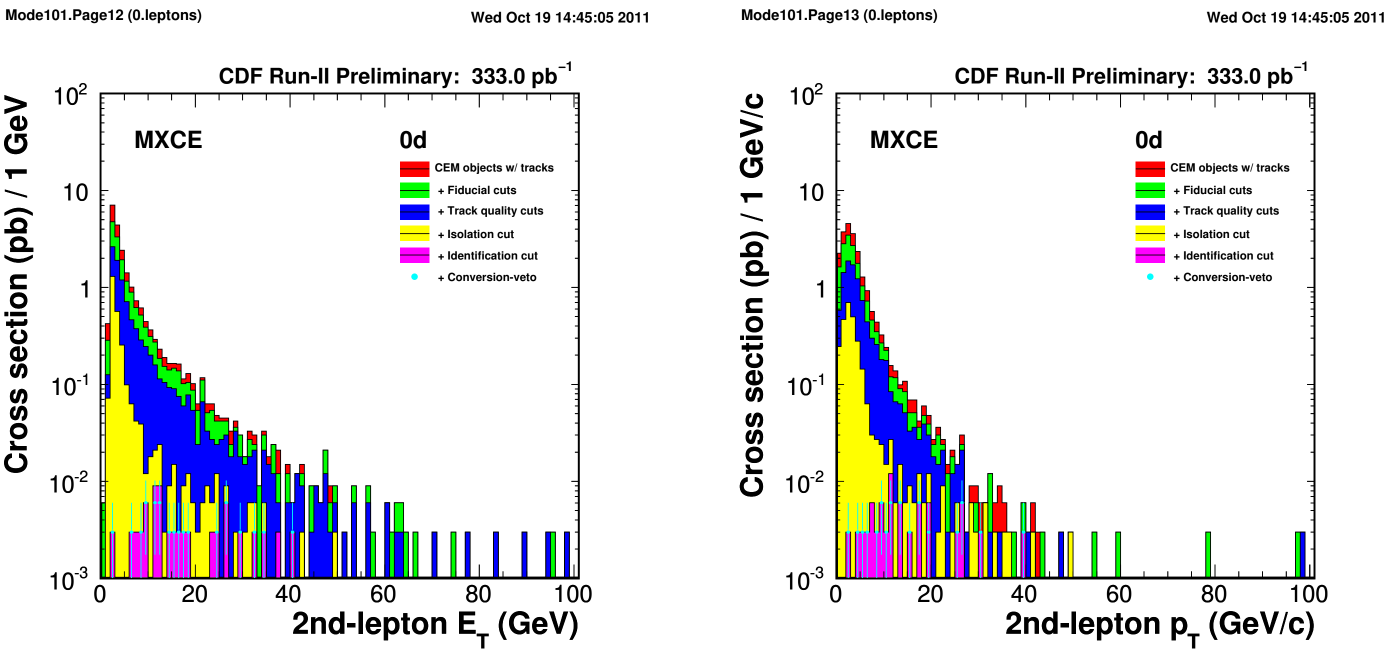

Figure 18: Inclusive E_T (left) and p_T (right) spectra for CEM objects with associated track(s) that are found in addition to the leading CMX muon from the `bhmu0d` dataset.

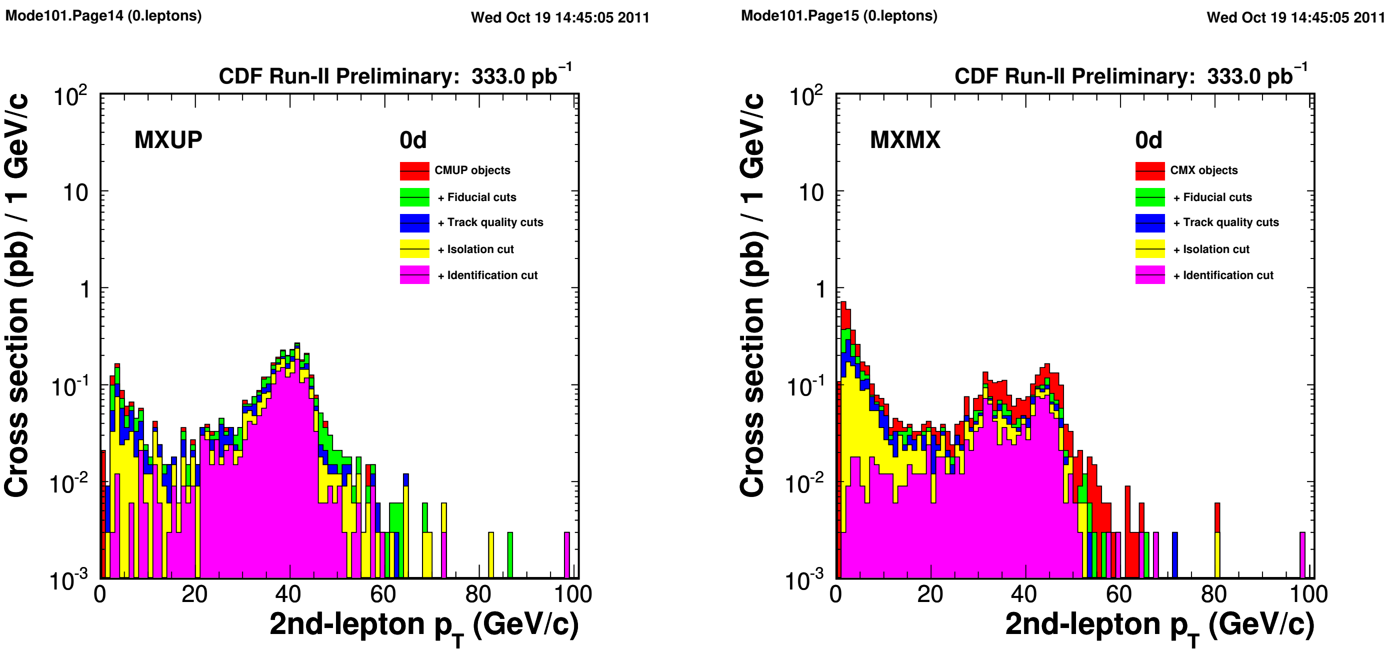

Figure 19: Inclusive p_T spectra for CMUP (left) and CMX (right) objects that are found in addition to the leading CMX muon from the `bhmu0d` dataset.

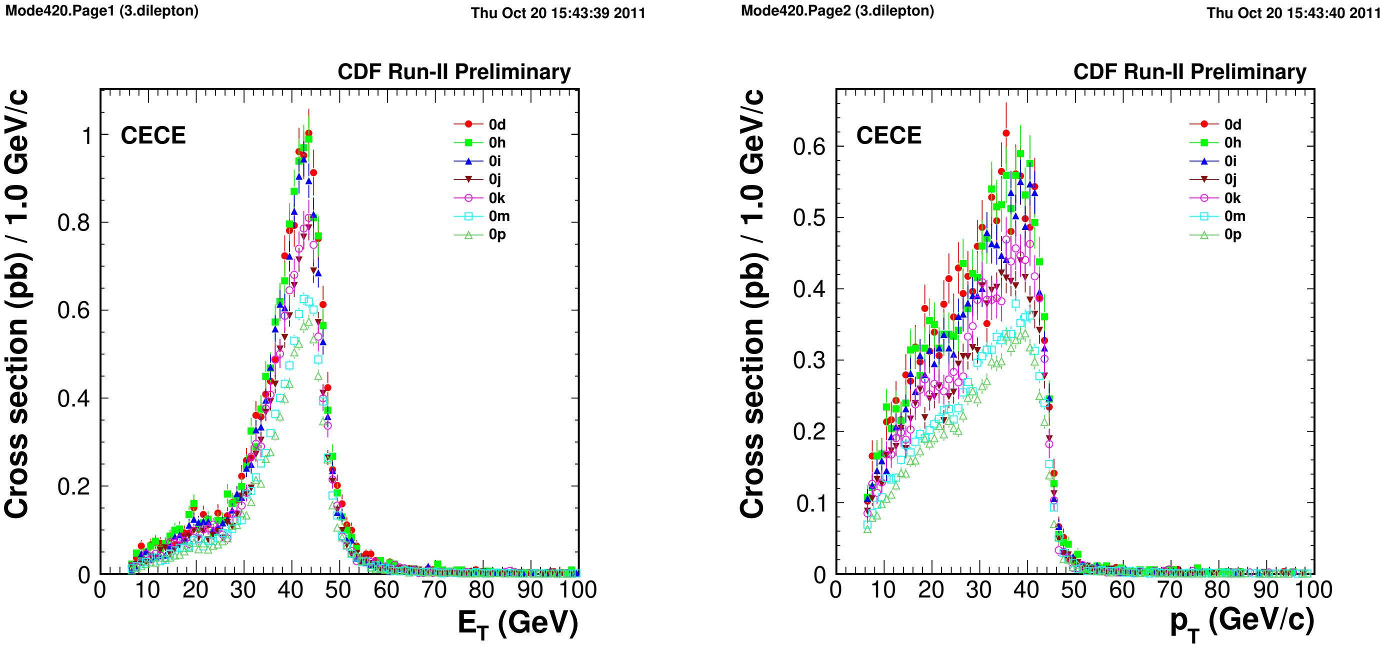

Figure 20: The E_T (left) and p_T (right) disributions for the 2nd CEM electron of dielectron events after all the baseline dilepton selection.

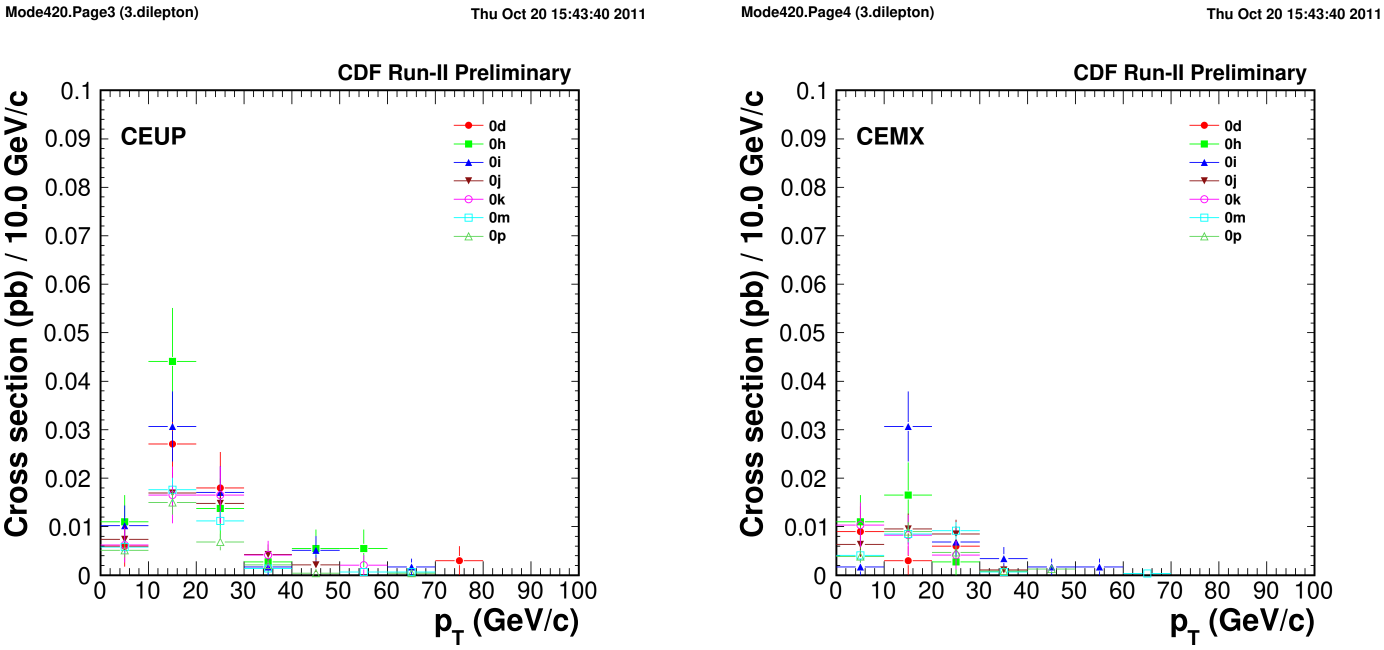

Figure 21: The p_T disributions for the 2nd leptons (muons) of $e\mu$ events after all the baseline dilepton selection. The left plot is CMUP and the right is CMX muons.

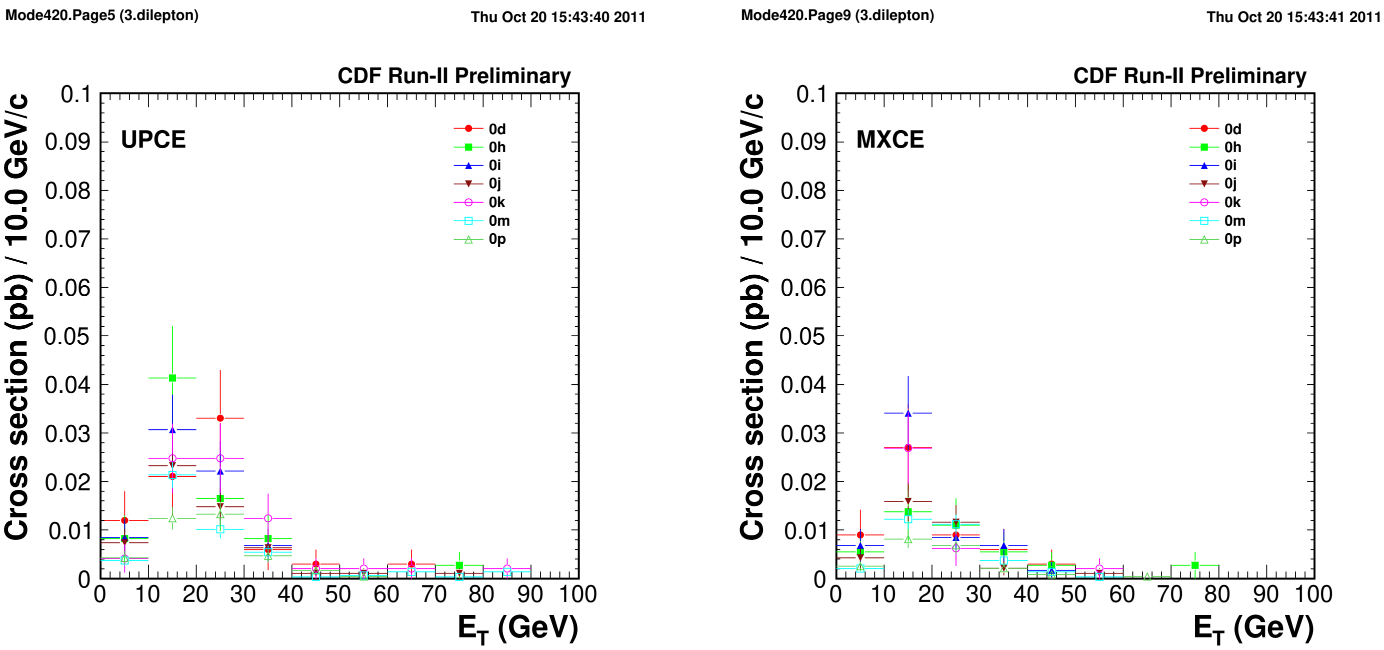

Figure 22: The E_T disributions for the 2nd leptons (electrons) of μe events after all the baseline dilepton selection. The left plot is CMUP-CE combination (UPCE) and the right is CMX-CE combination (MXCE).

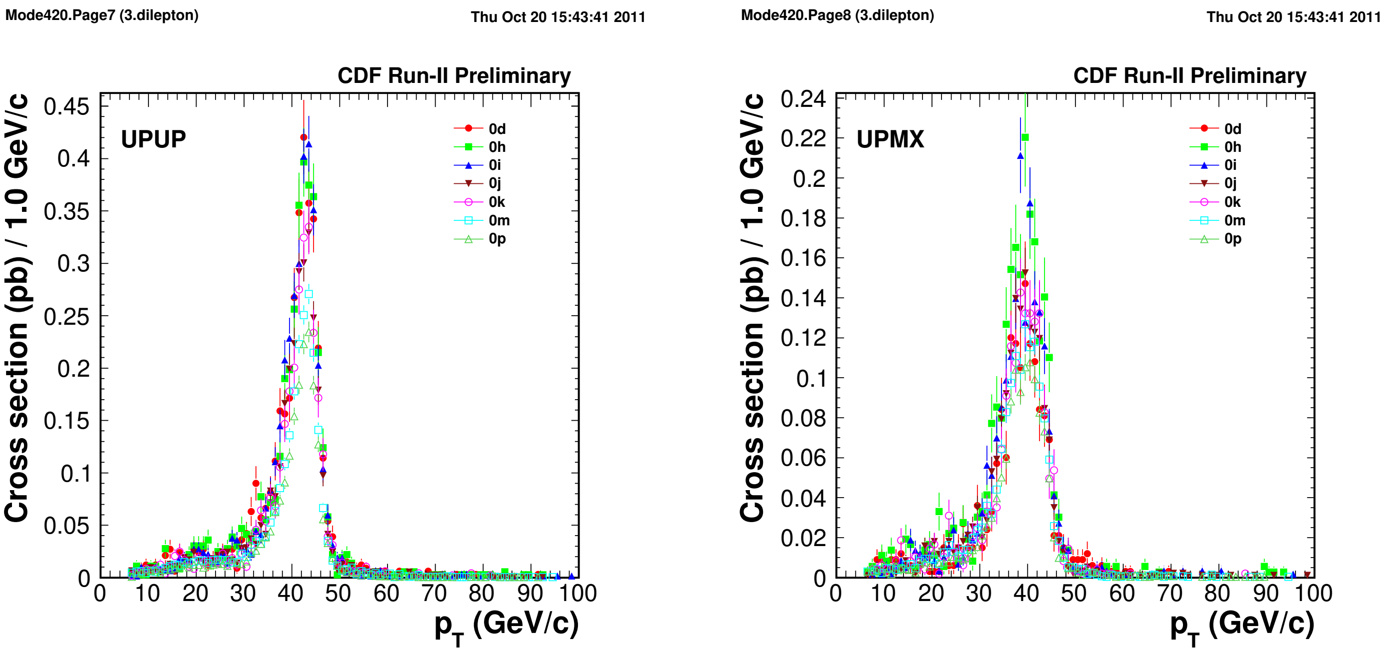

Figure 23: The p_T disributions for the 2nd muons of dimuon events after all the baseline dilepton selection. The left plot is CMUP-CMUP combination (UPUP) and the right is CMUP-CMX combination (UPMX).

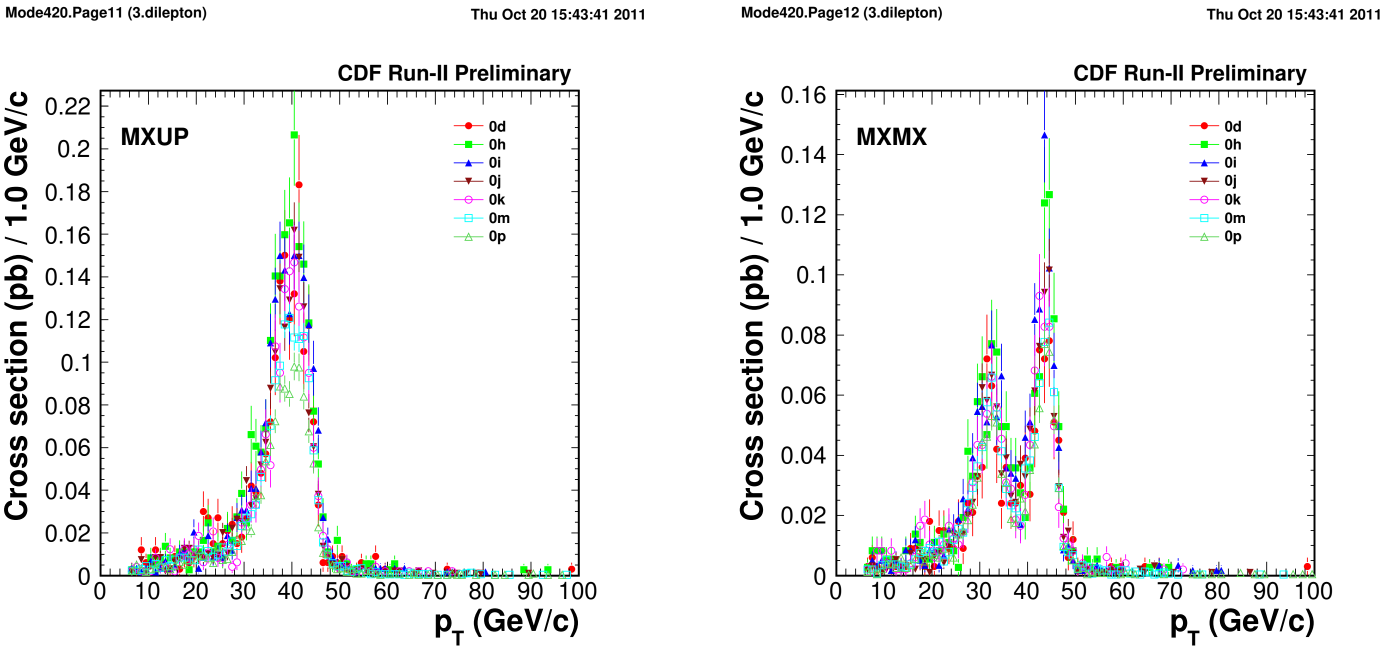

Figure 24: The p_T disributions for the 2nd muons of dimuon events after all the baseline dilepton selection. The left plot is CMX-CMUP combination (MXUP) and the right is CMX-CMX combination (MXMX).

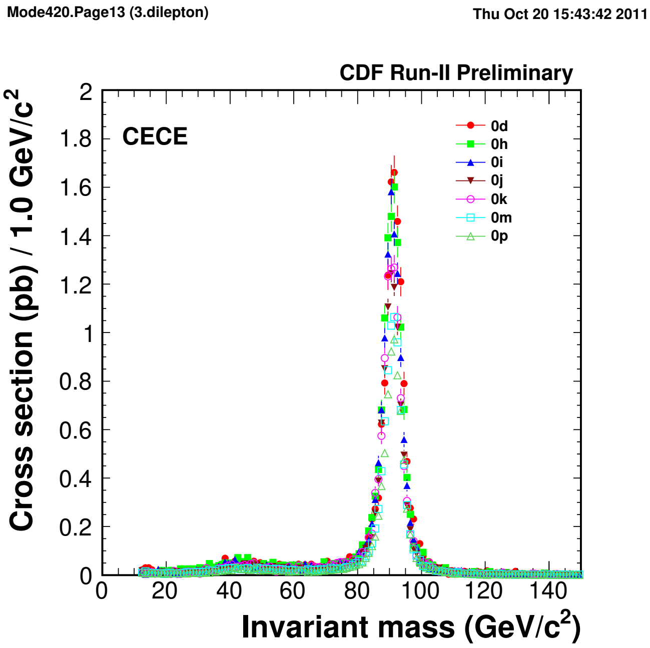

Figure 25: Invariant mass distribution of dielectron events after all the baseline dilepton selection.

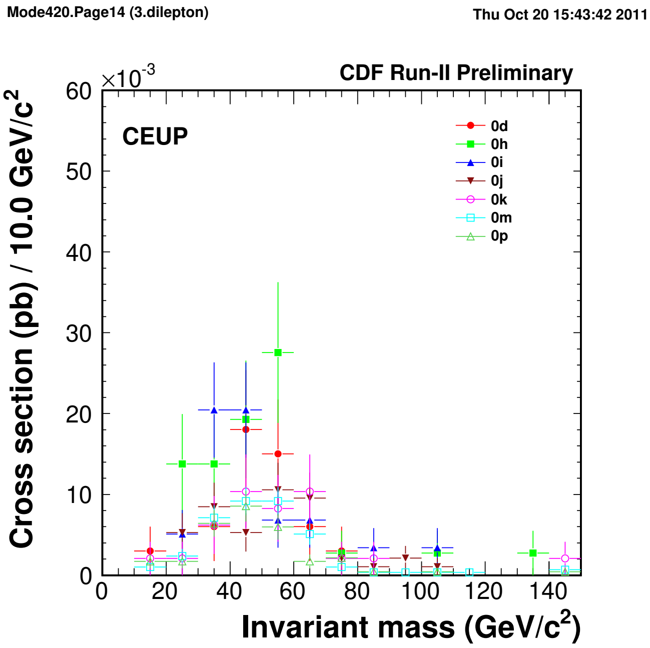

Figure 26: Invariant mass distribution of $e\mu$ events (CEM-CMUP combination) after all the baseline dilepton selection.

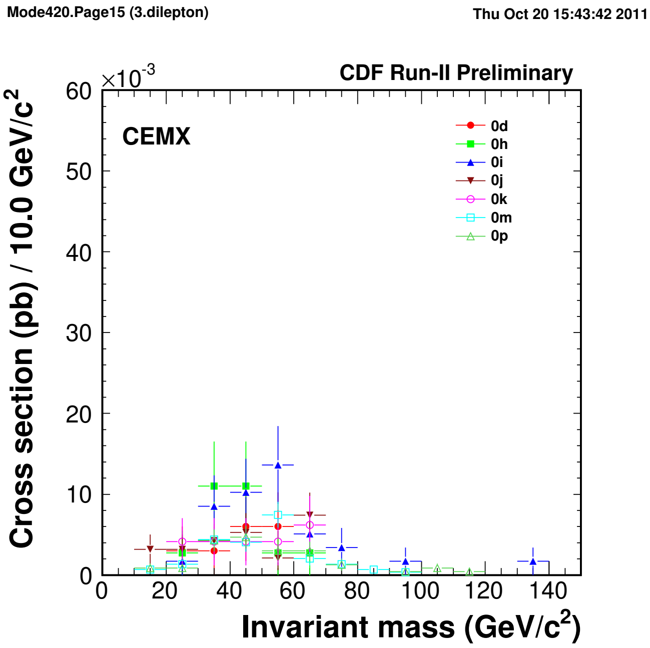

Figure 27: Invariant mass distribution of $e\mu$ events (CEM-CMX combination) after all the baseline dilepton selection.

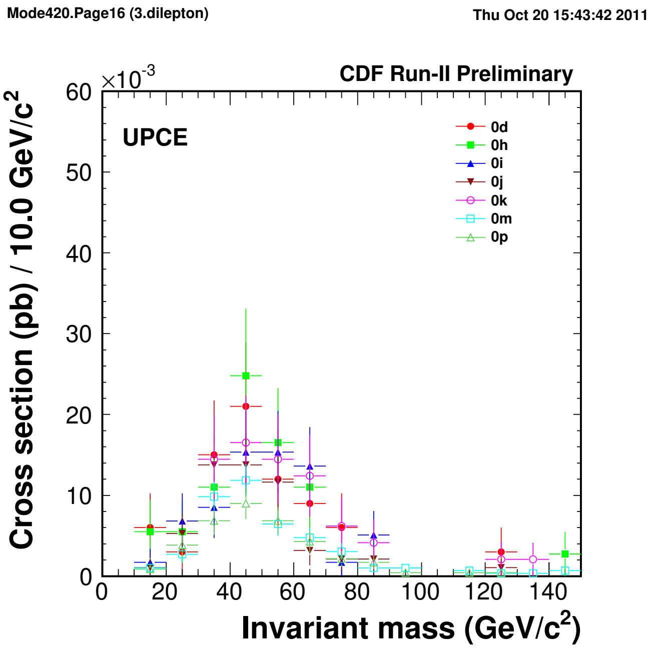

Figure 28: Invariant mass distribution of μe events (CMUP-CEM combination) after all the baseline dilepton selection.

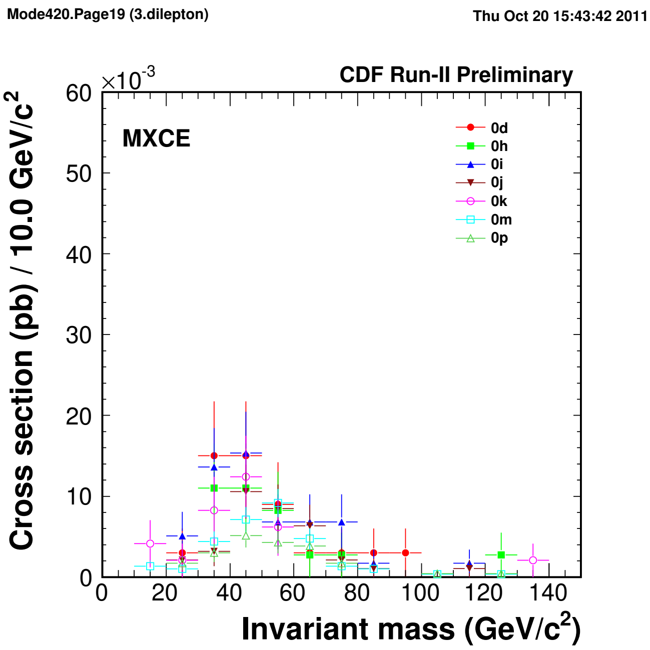

Figure 29: Invariant mass distribution of μe events (CMX-CEM combination) after all the baseline dilepton selection.

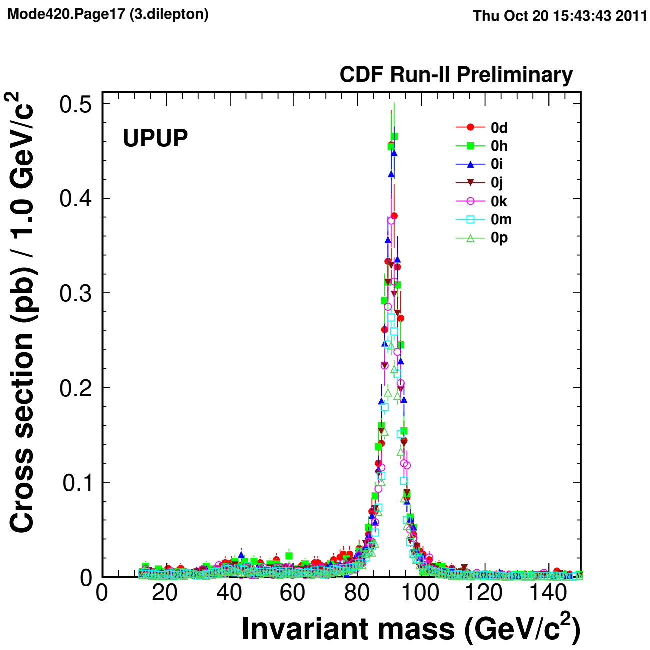

Figure 30: Invariant mass distribution of dimuon events (CMUP-CMUP combination) after all the baseline dilepton selection.

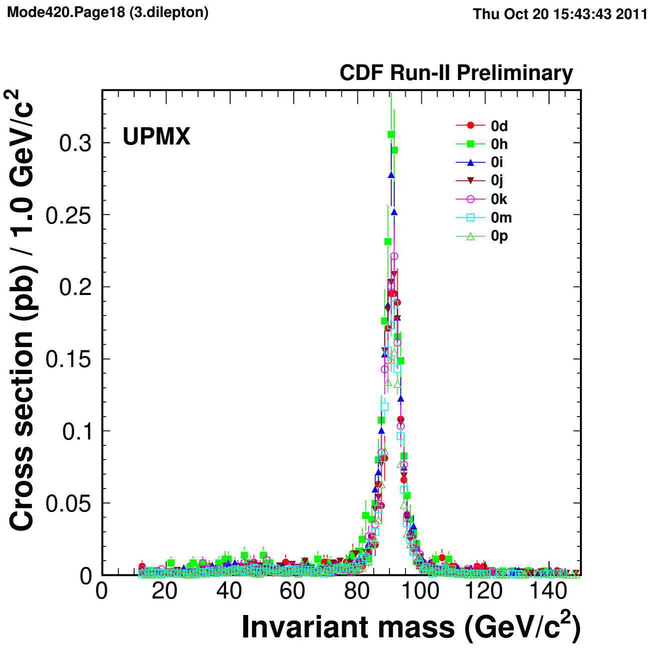

Figure 31: Invariant mass distribution of dimuon events (CMUP-CMX combination) after all the baseline dilepton selection.

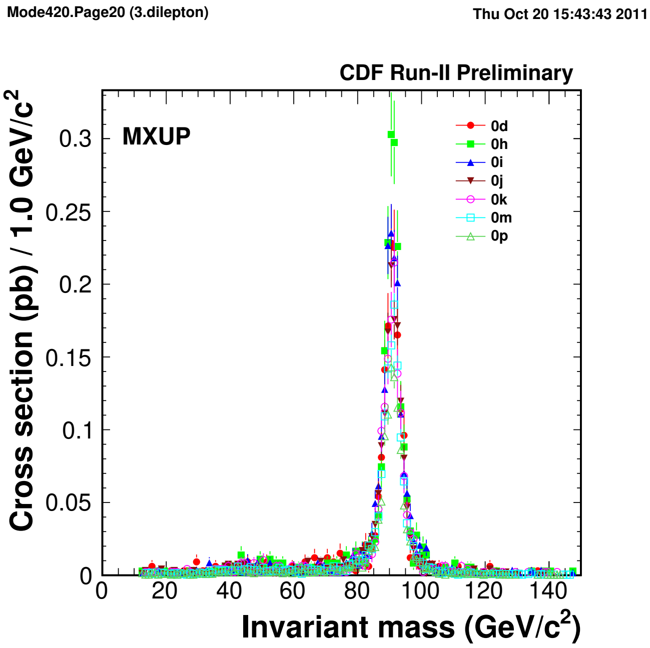

Figure 32: Invariant mass distribution of dimuon events (CMX-CMUP combination) after all the baseline dilepton selection.

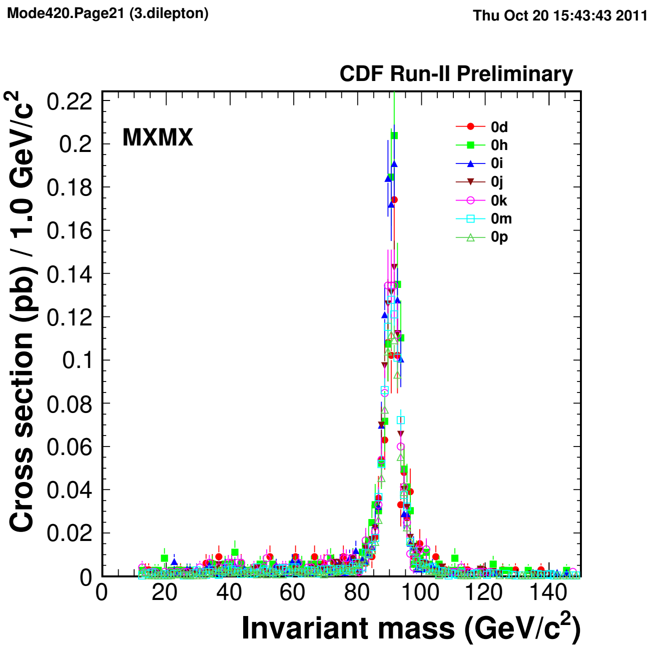

Figure 33: Invariant mass distribution of dimuon events (CMX-CMX combination) after all the baseline dilepton selection.

References

[1] Toru Okusawa, Yoshihiro Seiya, Takayuki Wakisaka, and Kazuhiro Yamamoto, "Baseline Selection of High-p_T Dilepton Events to Search for the Wh Production", CDF7260 (Version 3.0).

[2] A. Taffard, "Run II Cosmic Ray tagger", CDF6100.

[3] J. Nachtman, M. Worcester, and D. Saltzberg, "Background Estimation and Verification for the Like-Sign Dilepton Search", CDF6365.

[4] Toru Okusawa, Yoshihiro Seiya, Takayuki Wakisaka, Kazuhiro Yamamoto, Daisuke Yamato, and Mina Yoshida, "Likelihood-Based Lepton Identification to Search for the Vh Production", CDF10096 (Version 1.0).